NASA Technical Paper 1281

Effect of Concentration Dependence of the Diffusion Coefficient on Homogenization Kinetics in Multiphase Binary Alloy Systems

Darrel R. Tenney and Jalaiah Unnam

CASE FILE COPY

NOVEMBER 1978

NASA

NASA Technical Paper 1281

Effect of Concentration Dependence of the Diffusion Coefficient on Homogenization Kinetics in Multiphase Binary Alloy Systems

Darrel R. Tenney
Langley Research Center
Hampton, Virginia

and

Jalaiah Unnam
The George Washington University
Joint Institute for Advancement of Flight Sciences
Langley Research Center
Hampton, Virginia

National Aeronautics
and Space Administration

Scientific and Technical
Information Office

1978

SUMMARY

Diffusion calculations were performed to establish the conditions under which concentration dependence of the diffusion coefficient was important in single-, two-, and three-phase binary alloy systems. Finite-difference solutions for each type of system were obtained using diffusion coefficient variations typical of those observed in real alloy systems. Solutions were also obtained using average diffusion coefficients determined by taking a logarithmic average of each diffusion coefficient variation considered. The solutions for constant diffusion coefficients were used as references in assessing the effects of diffusion coefficient variations. Calculations were performed for planar, cylindrical, and spherical geometries in order to compare the effect of diffusion coefficient variations with the effect of interface geometries.

Diffusion coefficient variations in single-phase systems and in the major-alloy phase of two-phase systems were found to effect the kinetics of diffusion as strongly as the interfacial geometry of the diffusion couple. Concentration dependence of the diffusion coefficient in the minor-alloy phase of a two-phase system was found to have only an initial transient effect on the diffusion kinetics. In three-phase systems, the intermediate phase did not increase in thickness if the diffusion coefficient of the intermediate phase was smaller than the diffusion coefficient of the major-alloy phase. Under these conditions, the three-phase diffusion problem could be treated as a two-phase problem. However, if the diffusion coefficient of the intermediate phase was larger than the diffusion coefficient of the major-alloy phase, the intermediate phase grew rapidly at the expense of the major and minor phases. In most of the cases considered, the diffusion coefficient of the major-alloy phase was the key parameter that controlled the kinetics of interdiffusion.

INTRODUCTION

Solutions to the diffusion equation for a variety of initial and boundary conditions have been reported in the literature (refs. 1 to 7). Most of these, however, are restricted to planar geometry, are applicable only for infinite or semi-infinite systems, or require that the diffusion coefficient be constant. In treating diffusion in binary alloy systems, the assumption that the diffusion coefficient is constant is not always valid. Diffusion coefficient data for several single-phase and multiphase binary alloy systems show that an order of magnitude variation in the diffusion coefficient within a phase is not uncommon and in some cases, the diffusion coefficient may vary by as much as two orders of magnitude (refs. 8 to 12). A determination of the relative importance of the types and magnitudes of the diffusion coefficient variations found in real systems would provide an indication of the magnitude of the error associated with treating the diffusion coefficient as a constant.

The present study was undertaken to determine the relative importance of diffusion coefficient variations in single-, two-, and three-phase binary alloy

systems with planar, cylindrical, or spherical interfaces. Numerical solutions to the governing diffusion equations were obtained for various concentration-dependent diffusion coefficients as well as for two average (constant) diffusion coefficients. Two different methods of averaging were considered to determine the averaging method best suited for different types of diffusion coefficient variations. Solutions were also obtained for planar, cylindrical, and spherical geometries to compare the effects of interface geometries with those caused by concentration-dependent diffusion coefficients.

SYMBOLS

A,B	elements which constitute binary alloy system
C	concentration of sample, atomic fraction of B
$\bar{C}$	average concentration of sample, atomic fraction of B
C'	initial concentration of β-phase, assumed to be unity in this study, atomic fraction of B
C_o	initial concentration of α-phase, assumed to be zero in this study, atomic fraction of B
D	chemical diffusion coefficient (concentration dependent), m^2/sec
D^A	chemical diffusion coefficient of pure A, m^2/sec
D^B	chemical diffusion coefficient of pure B, m^2/sec
$D \uparrow$	designates a type of log linear D variation, D increases going away from interface, m^2/sec
$D \downarrow$	designates a type of log linear D variation, D decreases going away from interface, m^2/sec
$D \rightarrow$	designates a concentration-independent D whose value equals the logarithmic average of $D \uparrow$ or $D \downarrow$ variations considered in this study, m^2/sec
$\langle D \rangle$	designates a concentration-independent D whose value equals the integral average of $D \uparrow$ or $D \downarrow$ variations considered in this study, m^2/sec
H	amount of B in β-phase remaining at time t normalized to initial value for two- and three-phase systems; or amount of B remaining in original B-rich region at time t normalized to initial value for single-phase system
J	diffusion flux, $atoms/m^2/sec$

L	total thickness or diameter of specimen, m
ℓ	initial thickness or diameter of B-rich region, m
R	normalized distance, $r/(L/2)$
r	distance from center of B-rich region, m
s	interfacial surface area of B-rich material, m^2
t	time, sec
V_β^*	volume fraction of β-phase in specimen at equilibrium; other subscripts have similar meaning
v	volume of B-rich material, m^3
α,β	designations for terminal phases rich in A and B, respectively
γ	designation for intermediate phase
$\delta_{\beta\alpha}$	difference between solubility limits of β- and α-phases, $C_{\beta\alpha} - C_{\alpha\beta}$ (other double subscripts have similar meaning), atomic fraction of B
θ_D	temperature of interest, K
$\xi/2$	distance from center of β-phase to αβ interface in two-phase system, positive superscript designates α side of interface and negative superscript designates β side of interface, m
$\xi_1/2$	distance from center of β-phase to βγ interface in three-phase system, positive superscript designates γ side of interface and negative superscript designates β side of interface, m
$\xi_2/2$	distance from center of β-phase to αγ interface in three-phase system, positive superscript designates α side of interface and negative superscript designates γ side of interface, m

Superscripts:

α	A-rich phase
β	B-rich phase
γ	intermediate phase
*	denotes equilibrium value

Subscripts:

$\alpha\beta$	designates location in α-phase at	$\alpha\beta$	interface of two-phase system
$\alpha\gamma$	designates location in α-phase at	$\alpha\gamma$	interface of three-phase system
$\beta\alpha$	designates location in β-phase at	$\alpha\beta$	interface of two-phase system
$\beta\gamma$	designates location in β-phase at	$\beta\gamma$	interface of three-phase system
$\gamma\alpha$	designates location in γ-phase at	$\alpha\gamma$	interface of three-phase system
$\gamma\beta$	designates location in γ-phase at	$\beta\gamma$	interface of three-phase system

MATHEMATICAL ANALYSIS

The relationships between the binary phase diagrams and concentration profiles produced by diffusion between pure A and pure B after annealing for some intermediate time at temperature θ_D in single-, two-, and three-phase binary alloy systems are shown in figure 1. Figure 1(a) shows a continuous diffusion profile for a binary system A-B with complete solid solubility between A and B. Diffusion in a two-phase system with limited solid solubility produces a concentration profile (fig. 1(b)) with discontinuity at the $\alpha\beta$ interface equal to the difference between the solubility limits of the β- and α-phases $(C_{\beta\alpha} - C_{\alpha\beta})$. Diffusion in a three-phase system (limited solid solubility with intermediate phase formation) produces a concentration profile (fig. 1(c)) with discontinuities corresponding to the differences between the solubility limits of the β- and γ-phases $(C_{\beta\gamma} - C_{\gamma\beta})$ and the solubility limits of the γ- and α-phases $(C_{\gamma\alpha} - C_{\alpha\gamma})$.

Diffusion in these systems can be described by Fick's second law for each phase and by a flux-balance equation for each interface. Fick's second law is of the form

$$\frac{\partial C}{\partial t} = \frac{1}{r^m}\frac{\partial}{\partial r}\left(r^m D \frac{\partial C}{\partial r}\right) \tag{1}$$

where C is the atomic fraction of B, r is the distance from the center of B-rich region, D is the concentration-dependent diffusion coefficient, and m = 0, 1, or 2 for planar, cylindrical, or spherical geometries, respectively. The interface-flux-balance equation for the $\alpha\beta$ interface in the two-phase system is given by

$$(C_{\beta\alpha} - C_{\alpha\beta})\frac{d(\xi/2)}{dt} = D_{\alpha\beta}\left(\frac{dC^{\alpha}}{dr}\right)_{r=\xi^+/2} - D_{\beta\alpha}\left(\frac{dC^{\beta}}{dr}\right)_{r=\xi^-/2} \tag{2}$$

where $\xi/2$ is the location of the $\alpha\beta$ interface, with superscripts + and - designating the α and β sides of the interface, respectively. Two interface-flux-balance equations are required for the three-phase system. These are of the form

$$(C_{\beta\gamma} - C_{\gamma\beta})\frac{d(\xi_1/2)}{dt} = D_{\gamma\beta}\left(\frac{dC^{\gamma}}{dr}\right)_{r=\xi_1^+/2} - D_{\beta\gamma}\left(\frac{dC^{\beta}}{dr}\right)_{r=\xi_1^-/2} \tag{3}$$

at the $\beta\gamma$ interface and

$$(C_{\gamma\alpha} - C_{\alpha\gamma})\frac{d(\xi_2/2)}{dt} = D_{\alpha\gamma}\left(\frac{dC^{\alpha}}{dr}\right)_{r=\xi_2^+/2} - D_{\gamma\alpha}\left(\frac{dC^{\gamma}}{dr}\right)_{r=\xi_2^-/2} \tag{4}$$

at the $\alpha\gamma$ interface, where $\xi_1/2$ is the location of the $\beta\gamma$ interface with superscripts + and - denoting the γ and β sides of the interface, respectively, and $\xi_2/2$ is the location of the $\alpha\gamma$ interface with superscripts + and - denoting the α and γ sides of the interface, respectively. The initial and boundary conditions (fig. 2) to be satisfied for all three systems are

$$C = C' \qquad (0 \leqq r < \ell/2; \quad t = 0)$$

$$C = C_o \qquad (\ell/2 < r \leqq L/2; \quad t = 0)$$

$$\frac{\partial C}{\partial r} = 0 \qquad (r = 0 \text{ and } L/2; \quad t \geqq 0)$$

In this study, C' and C_o were assumed to be 1 and 0, respectively.

For two- and three-phase systems, all interface compositions were assumed equal to the equilibrium solubility limits of the phases. For a two-phase system at $\alpha\beta$ interface,

$$C = C_{\beta\alpha} \qquad (r = \xi^-/2)$$

$$C = C_{\alpha\beta} \qquad (r = \xi^+/2)$$

For a three-phase system at $\beta\gamma$ interface,

$$C = C_{\beta\gamma} \qquad (r = \xi_1^-/2)$$

$$C = C_{\gamma\beta} \qquad (r = \xi_1^+/2)$$

and at $\alpha\gamma$ interface,

$$C = C_{\gamma\alpha} \qquad (r = \xi_2^-/2)$$

$$C = C_{\alpha\gamma} \qquad (r = \xi_2^+/2)$$

Finite-difference analyses and computer programs were developed to solve the preceding equations. These solutions are applicable for planar, cylindrical, or spherical geometries with any size for the diffusion zone and any continuous variation (within a given phase) of the diffusion coefficient with concentration. Special techniques were included in the analyses to account for differences in molal volumes, initiation and growth of an intermediate phase (three-phase system), disappearance of a phase (two- and three-phase systems), and the presence of an initial composition profile in the specimen. A major improvement in solution accuracy was achieved in the two-phase analysis by employing a mass-conservation criterion to establish the location of the interface rather than the conventional interface-flux-balance criterion. In the three-phase analysis, computation time was minimized without sacrificing solution accuracy by treating the three-phase problem as a two-phase problem when the thickness of the intermediate phase was less than a small preset value. Three computer codes were developed to perform these analyses. Information concerning the availability of these codes and the essential features of each code, including a discussion of stability and accuracy, is found in reference 13.

Although the programs are general and can treat volume differences, the molal volumes and atomic weights of atoms A and B were assumed to be equal for the purposes of this paper. Thus, the concentration of B is the same whether expressed as atomic, weight, or volume fraction.

All three programs treat concentration dependence of the diffusion coefficient. Although any continuous variation of D (within a given phase) can be treated, only three types of D behavior were considered for this study: constant D, log D linearly increasing with C, and log D linearly decreasing with C. These cases were selected because of the experimentally observed trend for the log D to vary linearly with concentration (ref. 11). The change in D within a phase was assumed to be one of the three types: no change, one order of magnitude, and two orders of magnitude. Table 1 shows representative diffusion coefficient variations for several single-phase and multiphase binary alloy systems. The magnitude and variations of the diffusion coefficients chosen for this study are typical of values observed in metallic

systems above about two-thirds of the absolute melting point (ref. 14). The alloy phase thicknesses and exposure times were selected to yield concentration profiles which are typical of real systems, and to illustrate the effect of D variation on the diffusion kinetics.

RESULTS AND DISCUSSION

Single-Phase Systems

Effect of D variation.- Figure 3(a) shows the D variations studied for the single-phase system. The diffusion coefficient was assumed to vary linearly, on a log scale, with concentration. Four D variations were considered: (1) $D^B/D^A = 0.01$, (2) $D^B/D^A = 0.1$, (3) $D^B/D^A = 1$, and (4) $D^B/D^A = 100$, where D^B and D^A are the chemical diffusion coefficients of pure B and pure A, respectively. A summary of the conditions for which solutions were obtained is given in table 2. In all cases the radius or semithickness (L/2) of the couples was 150 μm.

Figure 3(b) shows the concentration profiles calculated for a cylindrical sample with $\bar{C} = 0.111$ using D of the form: (1) $D^B/D^A = 100$, (2) $D^B/D^A = 1$, and (3) $D^B/D^A = 0.01$ (cases 1, 2, and 3 of table 2). The exposure time shown was selected to give an intermediate stage of diffusion where distinct differences in the concentration profiles due to the different D variations were readily detectable. In the concentration region above 50 percent B, the concentration gradient dC/dr is largest for the $D^B/D^A = 0.01$ curve and smallest for the $D^B/D^A = 100$ curve. However, below 50 percent B the $D^B/D^A = 100$ variation curve has the largest gradient and the $D^B/D^A = 0.01$ curve the smallest. The concentration gradient tends to be largest where the diffusion coefficients are smallest, as expected.

Comparison of geometry and D variation effects.- Figure 4(a) shows the effect of D variation on the extent of diffusion for cylindrical geometry with $\bar{C} = 0.333$. The amount of B remaining in the original B-rich region, H, is plotted as a function of time for $D^B/D^A = 100$, 1, and 0.01 (cases 4, 5, and 6 of table 2). The curve for $D^B/D^A = 0.01$ approaches equilibrium value fastest because the value of D^A is higher than the D^A for the other two cases. In approaching equilibrium, the D values corresponding to compositions near pure A are important because of the absence of compositions near pure B for this high degree of homogenization. The time required to reach H = 0.50 was twice as long for the $D^B/D^A = 100$ case as for the $D^B/D^A = 0.01$ case.

Figure 4(b) shows the effect of interfacial geometry on the extent of diffusion for couples with $\bar{C} = 0.333$ and $D^B/D^A = 0.10$ (cases 7, 8, and 9 of table 2). The effect is as expected with diffusion taking place fastest for spherical geometry and slowest for planar geometry. Comparison of the curves in figure 4(b) with those in figure 4(a) suggests that the type of D variations observed in single-phase systems can be as important in determining the kinetics of interdiffusion as is the geometry of the sample.

Figure 5 shows the effect of interfacial geometry on the extent of diffusion for couples with $\bar{C} = 0.500$ and 0.010 (cases 10 to 12 and 13 to 15 of table 2). For high values of $\bar{C}$ (fig. 5(a)), diffusion proceeded fastest for spherical geometry and slowest for planar geometry. For low values of $\bar{C}$ (fig. 5(b)), just the opposite was true. An explanation of this switchover behavior is provided by the calculations presented in figure 6. The ratio s/v of interfacial surface area of B-rich material to its volume is shown for each geometry. These ratios are expressed in terms of $\bar{C}$ and L which were held constant in figures 5(a) and 5(b). The values of s/v are listed for $\bar{C} = 0.500$ and 0.010. As can be seen, planar geometry has the highest s/v of the three geometries for $\bar{C} = 0.010$ and spherical geometry has the highest s/v for $\bar{C} = 0.500$.

Two-Phase Systems

Effect of D variations.- The D variations shown in figure 7 were used to determine the effect of a concentration-dependent diffusion coefficient on interface motion and concentration profiles in two-phase systems. The D in the major-alloy phase α was assumed to vary linearly on a log scale with concentration. An increase in the diffusion coefficient of α in going from the interface composition to pure A has been denoted by $D^{\alpha}\uparrow$ and a decrease in the diffusion coefficient of α by $D^{\alpha}\downarrow$. This notation was adopted because it emphasizes the fact that the diffusion coefficients near the interface exert a greater influence on the diffusion kinetics than do the coefficients of the material away from the interface.

Two averages of the diffusion coefficient in the α-phase were considered; a logarithmic average $D^{\alpha}\rightarrow$, and an integral average $\langle D^{\alpha}\rangle$. These averages were calculated as follows:

$$(D^{\alpha}\rightarrow) = \exp\left[\frac{\int_0^{C_{\alpha\beta}} \ln D^{\alpha} dC}{\int_0^{C_{\alpha\beta}} dC}\right] = \sqrt{D_{\alpha\beta}\, D^{A}} = 10^{-14}\ \mathrm{m^2/sec} \tag{5}$$

$$\langle D^{\alpha}\rangle = \frac{\int_0^{C_{\alpha\beta}} D^{\alpha} dC}{\int_0^{C_{\alpha\beta}} dC} = \frac{D_{\alpha\beta} - D^{A}}{\ln\left(D_{\alpha\beta}/D^{A}\right)} = 1.236 \times 10^{-14}\ \mathrm{m^2/sec} \tag{6}$$

where $D_{\alpha\beta}$ and D^{A} are the diffusion coefficients corresponding to the composition of the interface $C_{\alpha\beta}$ and to pure A, respectively.

The combinations of D^{α} and D^{β} for which calculations were performed are listed in table 3. The specimen geometry, initial radius (or semithickness) of the β-phase region, and average composition of the sample $\bar{C}$ are also tabulated for each case considered. The diffusion coefficient in the minor-alloy phase β was held constant. Also, the solubility limits of the β- and α-phases, $C_{\beta\alpha}$ and $C_{\alpha\beta}$, were held constant.

A plot of the normalized thickness of the β-phase versus square root of the exposure time for $\bar{C} = 0.02$ (cases 1, 2, 3, and 4 of table 3) is shown in figure 8(a). The fastest rate of interface motion occurred for $D^{\alpha}\downarrow$ and the slowest for $D^{\alpha}\uparrow$ because the diffusion coefficient near the interface is highest for the $D^{\alpha}\downarrow$ variation and lowest for the $D^{\alpha}\uparrow$ variation. The $D^{\alpha}\rightarrow$ variation produced interface motion similar to the $D^{\alpha}\uparrow$ variation, whereas the $\langle D^{\alpha}\rangle$ produced interface motion more nearly like that of $D^{\alpha}\downarrow$. Thus, the best average diffusion coefficient for a $D^{\alpha}\uparrow$ variation is a logarithmic average (eq. (5)), and for a $D^{\alpha}\downarrow$ variation, an integral average is best (eq. (6)).

Figure 8(b) shows concentration profiles at $\sqrt{t} = 300\ \mathrm{sec}^{1/2}$, calculated for cases 1, 2, and 4 of table 3. Saturation of the β-phase occurs early because the β-phase is thin relative to the α-phase and the diffusion coefficients are approximately the same in each phase. After the β-phase saturates, it will decrease in thickness at a rate controlled by diffusion in the α-phase. The concentration gradient in the α-phase near the interface is steepest for $D^{\alpha}\uparrow$ because of the low $D_{\alpha\beta}$. The curves for $D^{\alpha}\downarrow$ and $D^{\alpha}\uparrow$ crossover away from the interface because, as the concentration tends to pure A, the diffusion coefficients for $D^{\alpha}\uparrow$ are higher than those for $D^{\alpha}\downarrow$.

The extent of interdiffusion for a cylindrical couple with $\bar{C} = 0.20$ is shown in figure 9 where ξ/ℓ and H (normalized amount of B in the β-phase) are plotted as a function of $\sqrt{t}$. Both plots show essentially the same behavior with equilibrium being established at a ξ/ℓ value of 0.598 and an H value of 0.304. Both α- and β-phases are present in the sample at equilibrium because $\bar{C} = 0.20$ lies in the $\alpha + \beta$ region.

Comparison of geometry and D variation effects.- A comparison of the effects due to differences in geometry and in D variations for a two-phase system is shown in figure 10. The results indicate that typical D^{α} variations can have a greater influence on the kinetics of interdiffusion than the geometry of the interface. Comparison of the results of figure 10 for a two-phase sample with the results of figure 4 for a single-phase sample reveals that D variations in two-phase systems can be as important as D variations in single-phase systems.

Three-Phase Systems

The type of diffusion behavior observed in three-phase systems is dependent on solubilities of each phase, rates of diffusion in each phase, and initial thicknesses of the α- and β-phases, and therefore the average composition of the diffusion couple $\bar{C}$. If $\bar{C}$ lies in one of the single-phase

regions, only that phase will remain at equilibrium. If $\bar{C}$ lies in the $\alpha + \gamma$ region, the equilibrium volume fractions of γ- and α-phases are given by

$$V_{\gamma}^{*} = \frac{\bar{C} - C_{\alpha\gamma}}{C_{\gamma\alpha} - C_{\alpha\gamma}}$$

and

$$V_{\alpha}^{*} = 1 - V_{\gamma}^{*}$$

In this study, $\bar{C}$ was chosen to be in the α region or the $\alpha + \gamma$ region.

Concentration profiles.- The principal effects of the solubility limits and $\bar{C}$ are, to a large extent, predictable from the equilibrium phase diagram. However, the effects of unequal rates of diffusion in each phase and variations in the diffusion coefficient within a given phase are not discernible from the phase diagram. For this reason, the primary emphasis of this study was placed on characterizing the effect of the different diffusion coefficients and their variations on the dissolution characteristics. The D variations investigated in this study are illustrated in figure 11. The different D combinations considered are listed in table 4 along with $\bar{C}$ and the solubility limits. These cases were selected because they represent typical parameters for real systems. The designations for D variations ($D \rightarrow$, $D \uparrow$, $D \downarrow$, and $\langle D \rangle$) are the same as the ones discussed for two-phase systems.

The concentration profiles calculated for a cylindrical couple with $\bar{C} = 0.02$ (case 1 of table 4) are shown in figure 12. The three profiles illustrate the major concentration and phase changes occurring during the initial and intermediate stages of diffusion. Because the β-phase is thin relative to the α-phase, diffusion proceeds to the center of the β-phase early in the diffusion process resulting in a reduction in the concentration gradient in the β-phase. The intermediate γ-phase does not significantly increase in thickness until the concentration gradient in the β-phase approaches zero. From this time on, the γ-phase grows at the expense of the β-phase until the β-phase is totally consumed. The γ-phase will then decrease in thickness and disappear with only the α-phase remaining at complete homogenization. The sequence of events is controlled by solubilities, initial volume fractions, and diffusion coefficients. The effect of each of these variables on the diffusion process will be discussed in the following sections with primary emphasis placed on the effect of diffusion coefficient variations on the motion of phase boundaries.

Effect of relative magnitude and variation of D in the major-alloy phase.- Solutions were determined for $D^{\alpha}\downarrow$, $D^{\alpha}\uparrow$, $D^{\alpha}\rightarrow$, and $\langle D^{\alpha} \rangle$ assuming D^{β} and D^{γ} to be constant and equal to $D^{\alpha}\rightarrow$ (cases 1, 2, 3, and 4 of table 4). The results for the normalized thickness of the β-phase are shown in figure 13 as a function of $\sqrt{t}$. The curves in this figure have the same general behavior as those presented in figure 8(a) (same $\bar{C}$, geometry, D variations, and

terminal phase solubilities) for the two-phase sample. The principal difference in the two sets of curves is that, in the three-phase system, the β-phase disappears in a shorter time and the spread between the D variation curves is not as large. The faster rate of loss of β in the three-phase system is due to its low solubility gap ($\delta_{\beta\gamma}$ = 0.85 - 0.51 = 0.34) when compared to the two-phase value ($\delta_{\beta\alpha}$ = 0.85 - 0.15 = 0.70), requiring less material transport for the β to γ transformation with respect to β to α transformation. The spread between the D variation curves in a three-phase system is smaller because the intermediate γ-phase damps the effect of the D^{α} variation. This damping effect coupled with lower solubility limits makes the D^{α} variations in three-phase systems less important than in two-phase systems.

The sensitivity of the diffusion process to large differences in the value of D^{α} (with respect to D^{β} and D^{γ}) is illustrated in figure 14. The conditions for these calculations are summarized in table 4 (cases 5, 6, and 7). When D^{α} was high $\left((D^{\alpha}\rightarrow) \times 100\right)$, the thickness of the β-phase decreased rapidly until the α-phase saturated (fig. 14(a)). The concentration profiles shown in figure 14(b) indicate that at $\sqrt{t}$ = 50 $sec^{1/2}$, the α-phase is saturated for the $(D^{\alpha}\rightarrow) \times 100$ case. Once the α-phase saturates, the kinetics are primarily controlled by diffusion in the γ-phase because the solubility of β-phase is only 1 percent.

Effect of relative magnitude of D in minor-alloy phase.- Because D variations in the minor-alloy phase are less important than in the major-alloy phase and would, in the worst case, have only an initial transient effect, only order of magnitude changes in the diffusion coefficient of the minor-alloy phase were studied (cases 1, 8, and 9 of table 4). The normalized thicknesses of the β- and γ-phases are shown in figure 15 as a function of $\sqrt{t}$. The change in thickness of the γ-phase, $(\xi_2 - \xi_1)/\ell$, was not significantly affected by the value of D^{β}. The value of D^{β} has only an initial transient effect on the thickness of the β-phase, (ξ_1/ℓ). Once the β-phase saturates, the value of D^{β} is unimportant because D^{γ} and D^{α} then control the diffusion process.

Effect of relative magnitude of D in the intermediate phase.- Because intermediate phases in binary alloy systems generally have small solubility ranges (less than 0.05, atomic fraction B), concentration dependence of diffusion coefficients in these phases is not significant. Therefore, in studying the effect of the diffusion coefficient of the intermediate phase D^{γ} on the diffusion kinetics, only order of magnitude changes in D^{γ} were considered. Figure 16 shows the results for cases 1, 10, and 11 of table 4. When D^{γ} was low $\left((D^{\gamma}\rightarrow)/100\right)$, the γ-phase did not grow in thickness, and the rate of loss of β-phase was less than for $D^{\gamma}\rightarrow$. Under these conditions, computation time is minimized (without sacrificing solution accuracy) by analytically treating the three-phase problem as a two-phase problem. When D^{γ} was high $\left((D^{\gamma}\rightarrow) \times 100\right)$, the γ-phase grew rapidly at the expense of both α and β; this resulted in a rapid decrease in the β-phase thickness. Concentration profiles for $\sqrt{t}$ = 50 $sec^{1/2}$ are shown in figure 16(b) for all three D^{γ} values. The profile for $(D^{\gamma}\rightarrow) \times 100$ shows that the γ-phase grew into the initial β-phase region much faster than into the α-phase because of the early saturation of the β-phase. The γ-phase will increase in thickness until β disappears and then decrease in thickness until it disappears leaving only α-phase in the specimen.

Figure 17 shows the results for $\bar{C} = 0.40$ (cases 5, 12, and 13 of table 4). Although $\bar{C}$ and solubilities are different from those used to calculate the curves shown in figure 16, the same general behavior is observed. If D^{γ} is less than or equal to D^{α} and D^{β}, the kinetics are primarily controlled by diffusion in the α-phase. However, if D^{γ} is larger than D^{α} and D^{β}, the kinetics are dominated in the early stages by the growth of the γ-phase. Therefore, intermediate phases in three-phase systems are unlikely to act as suitable diffusion barriers between the terminal phases.

CONCLUDING REMARKS

Diffusion calculations were performed to establish the conditions under which concentration dependence of the diffusion coefficient was important in single-, two-, and three-phase binary alloy systems. Finite-difference solutions for each type of system were obtained using diffusion coefficient variations typical of those observed in real alloy systems. Solutions were also obtained using average diffusion coefficients and used as reference in assessing the effects of diffusion coefficient variations. Calculations were performed for planar, cylindrical, and spherical geometries in order to compare the effect of diffusion coefficient variations with the effect of interface geometries. Based on the results obtained, the following conclusions were drawn.

Single-Phase Systems

1. Concentration dependence of the diffusion coefficient in single-phase systems was found to affect the kinetics of diffusion as strongly as the interfacial geometry of the diffusion couple.

2. The influence of geometry and average composition of the couple ($\bar{C}$, atomic fraction B) on diffusion kinetics is related to the ratio of interfacial surface area of B-rich material to its volume.

Two-Phase Systems

1. Concentration dependence of the diffusion coefficient in the major-alloy phase of a two-phase system affects the kinetics of diffusion as strongly as the interfacial geometry of the diffusion couple.

2. The diffusion coefficients of the compositions close to the solubility limits exert a greater influence on the diffusion kinetics than do the coefficients of the compositions further away from the interface.

3. The integral average gives a better representation of the major-alloy phase diffusion coefficient D^{α} when D^{α} decreases in going from the interfacial composition toward pure material. The logarithmic average gives a better representation of D^{α} variation when D^{α} increases in going from the interfacial composition toward pure material.

Three-Phase Systems

1. Concentration dependence of the diffusion coefficient is significant only for the major-alloy phase. The damping effect of the intermediate phase makes the effect of diffusion coefficient variations on minor-phase thickness less important with respect to the two-phase system for comparable conditions.

2. Two orders of magnitude change in the diffusion coefficient of the minor-alloy phase for a sample with $\bar{C} = 0.02$ had only an initial transient effect on the kinetics of diffusion.

3. The diffusion coefficient of the intermediate phase D^{γ} has significant effect on the diffusion kinetics only when D^{γ} is greater than the diffusion coefficients of the terminal phases.

4. When D^{γ} is small relative to the diffusion coefficients of the terminal phases, the intermediate phase remains extremely thin during the initial stages of diffusion. Under these conditions, computation time is minimized (without sacrificing solution accuracy) by analytically treating the three-phase problem as a two-phase problem.

5. Intermediate phases in three-phase systems are unlikely to act as suitable diffusion barriers between the terminal phases.

Langley Research Center
National Aeronautics and Space Administration
Hampton, VA 23665
August 25, 1978

REFERENCES

1. Tanzilli, R. A.; and Heckel, R. W.: Numerical Solutions to the Finite, Diffusion-Controlled, Two-Phase, Moving-Interface Problem (With Planar, Cylindrical, and Spherical Interfaces). Trans. Met. Soc. AIME, vol. 242, no. 11, Nov. 1968, pp. 2313-2321.

2. Tanzilli, R. A.; and Heckel, R. W.: An Analysis of Interdiffusion in Finite-Geometry, Two-Phase Diffusion Couples in the Ni-W and Ag-Cu Systems. Metall. Trans., vol. 2, no. 7, July 1971, pp. 1779-1784.

3. Lanam, R. D.; and Heckel, R. W.: A Study of the Effect of an Intermediate Phase on the Dissolution and Homogenization Characteristics of Binary Alloys. Metall. Trans., vol. 2, no. 8, Aug. 1971, pp. 2255-2266.

4. Unnam, J.; and Houska, C. R.: Iterative and Finite Difference Computer Programs for Diffusion in Single and Two Phase Systems. Grant No. NSF-GH-30180A #1, Virginia Polytech. Inst. & State Univ., Jan. 1976. (Available from NTIS as PB-256 282.)

5. Houska, C. R.; and Unnam, J.: Iterative Approaches Describing Atomic Diffusion in Finite Single- and Two-Phase Systems. J. Appl. Phys., vol. 47, no. 10, Oct. 1976, pp. 4325-4335.

6. Herring, Harvey W.; and Tenney, Darrel R.: Diffusion in a Unidirectional Filament Reinforced Metal Composite. Metall. Trans., vol. 4, no. 2, Feb. 1973, pp. 437-441.

7. Tenney, Darrel R.: Diffusion Analysis for Two-Phase Metal-Matrix Composite. NASA TN D-8299, 1976.

8. Tenney, Darrel R.; and Talty, Patrick K.: X-Ray Diffraction Investigation of Bimetallic Diffusion Zones in the Cu-Pd System. Metall. Trans., vol. 5, no. 1, Jan. 1974, pp. 241-247.

9. Unnam, J.; Carpenter, J. A.; and Houska, C. R.: X-Ray Diffraction Approach to Grain Boundary and Volume Diffusion. J. Appl. Phys., vol. 44, no. 5, May 1973, pp. 1957-1967.

10. Unnam, J.; and Houska, C. R.: An X-Ray Study of Diffusion in the Cu-Ag System. J. Appl. Phys., vol. 47, no. 10, Oct. 1976, pp. 4336-4342.

11. Smithells, Colin J.: Metals Reference Book - Volume II. Fourth ed. Plenum Press, 1967.

12. Svechnikov, V. N., ed.: Diffusion Processes in Metals. TT 70-50030, Nat. Bur. Stand. and Nat. Sci. Found., c.1970.

13. Tenney, Darrel R.; and Unnam, Jalaiah: Numerical Analyses for Treating Diffusion in Single-, Two-, and Three-Phase Binary Alloy Systems. NASA TM-78636, 1978.

14. Seith, Wolfgang; and Heumann, Theodor: Diffusion of Metals: Exchange Reactions. Second ed., AEC-tr-4506, U.S. At. Energy Comm., 1955.

TABLE 1.- DIFFUSION COEFFICIENT VARIATIONS FOR SEVERAL SINGLE-PHASE AND MULTIPHASE BINARY ALLOY SYSTEMS

System, A-B	Temp., K	Composition range, atomic fraction B	$\frac{\text{Max. } D}{\text{Min. } D}$	No. of phases	Reference
Cu-Ni	1173	0-1.00	100	1	9
Ni-Pd	1292	0-1.00	17	1	12 (p. 52)
Cu-Pd	1173	0-1.00	25	1	8
Nb-W	2373	0-1.00	100	1	11 (p. 679)
Ag-Cu	1023	0-0.12 Cu	10	2	10
Mo-Ti	1123	0.10-0.90 Ti	10	2	12 (p. 39)
Ag-Zn	883	0.40-0.55 Zn	20	5	11 (p. 674)
Fe-Al	1123	0-0.18 Al	15	6	11 (p. 675)

TABLE 2.- CASES CONSIDERED FOR SINGLE-PHASE SYSTEM

[$L/2 = 150$ μm]

No.	Geometry	(D^B/D^A)	$\bar{C}$	$(\ell/2)$, μm
1	Cylindrical	100	0.111	50
2	Cylindrical	1	.111	50
3	Cylindrical	.01	.111	50
4	Cylindrical	100	.333	86.6
5	Cylindrical	1	.333	86.6
6	Cylindrical	.01	.333	86.6
7	Cylindrical	.10	.333	86.6
8	Planar	.10	.333	50
9	Spherical	.10	.333	104
10	Planar	1	.500	75
11	Cylindrical	1	.500	106.1
12	Spherical	1	.500	119.1
13	Planar	1	.010	1.5
14	Cylindrical	1	.010	15
15	Spherical	1	.010	32.3

TABLE 3.- CASES CONSIDERED FOR TWO-PHASE SYSTEM

$\left[C_{\beta\alpha} = 0.85, \quad C_{\alpha\beta} = 0.15, \quad L/2 = 140\ \mu m\right]$

No.	Geometry	D^{α}	D^{β}	$\bar{C}$	$(\ell/2)$, μm
1	Cylindrical	$D^{\alpha}\downarrow$	$D^{\beta}\rightarrow$	0.02	20.0
2	Cylindrical	$D^{\alpha}\uparrow$	$D^{\beta}\rightarrow$	.02	20.0
3	Cylindrical	$D^{\alpha}\rightarrow$	$D^{\beta}\rightarrow$	.02	20.0
4	Cylindrical	$\langle D^{\alpha}\rangle$	$D^{\beta}\rightarrow$	.02	20.0
5	Cylindrical	$D^{\alpha}\downarrow$	$D^{\beta}\rightarrow$	.20	62.6
6	Cylindrical	$D^{\alpha}\uparrow$	$D^{\beta}\rightarrow$	.20	62.6
7	Cylindrical	$D^{\alpha}\rightarrow$	$D^{\beta}\rightarrow$	.20	62.6
8	Cylindrical	$\langle D^{\alpha}\rangle$	$D^{\beta}\rightarrow$	.20	62.6
9	Planar	$D^{\alpha}\rightarrow$	$D^{\beta}\rightarrow$	.20	28.0
10	Spherical	$D^{\alpha}\rightarrow$	$D^{\beta}\rightarrow$	.20	81.9

TABLE 4.- CASES CONSIDERED FOR THREE-PHASE SYSTEM

[Cylindrical geometry, $C_{\gamma\beta} = 0.51$, $C_{\gamma\alpha} = 0.49$]

No.	D^{α}	D^{β}	D^{γ}	$C_{\beta\gamma}$	$C_{\alpha\gamma}$	$\bar{C}$	$(\ell/2)$, μm	$(L/2)$, μm
1	$D^{\alpha}\rightarrow$	$D^{\beta}\rightarrow$	$D^{\gamma}\rightarrow$	0.85	0.15	0.02	20	140
2	$D^{\alpha}\downarrow$	$D^{\beta}\rightarrow$	$D^{\gamma}\rightarrow$	.85	.15	.02	20	140
3	$D^{\alpha}\uparrow$	$D^{\beta}\rightarrow$	$D^{\gamma}\rightarrow$	.85	.15	.02	20	140
4	$\langle D^{\alpha}\rangle$	$D^{\beta}\rightarrow$	$D^{\gamma}\rightarrow$	.85	.15	.02	20	140
5	$D^{\alpha}\rightarrow$	$D^{\beta}\rightarrow$	$D^{\gamma}\rightarrow$	.99	.20	.40	50	79
6	$(D^{\alpha}\rightarrow) \times 100$	$D^{\beta}\rightarrow$	$D^{\gamma}\rightarrow$	.99	.20	.40	50	79
7	$(D^{\alpha}\rightarrow)/100$	$D^{\beta}\rightarrow$	$D^{\gamma}\rightarrow$	.99	.20	.40	50	79
8	$D^{\alpha}\rightarrow$	$(D^{\beta}\rightarrow) \times 100$	$D^{\gamma}\rightarrow$	.85	.15	.02	20	140
9	$D^{\alpha}\rightarrow$	$(D^{\beta}\rightarrow)/100$	$D^{\gamma}\rightarrow$	.85	.15	.02	20	140
10	$D^{\alpha}\rightarrow$	$D^{\beta}\rightarrow$	$(D^{\gamma}\rightarrow) \times 100$	.85	.15	.02	20	140
11	$D^{\alpha}\rightarrow$	$D^{\beta}\rightarrow$	$(D^{\gamma}\rightarrow)/100$	.85	.15	.02	20	140
12	$D^{\alpha}\rightarrow$	$D^{\beta}\rightarrow$	$(D^{\gamma}\rightarrow) \times 100$	.99	.20	.40	50	79
13	$D^{\alpha}\rightarrow$	$D^{\beta}\rightarrow$	$(D^{\gamma}\rightarrow)/100$	.99	.20	.40	50	79

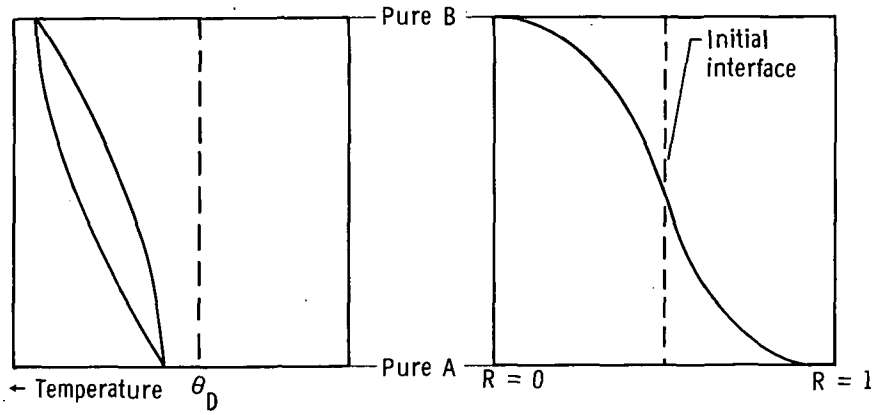

(a) Single phase - complete solid solubility.

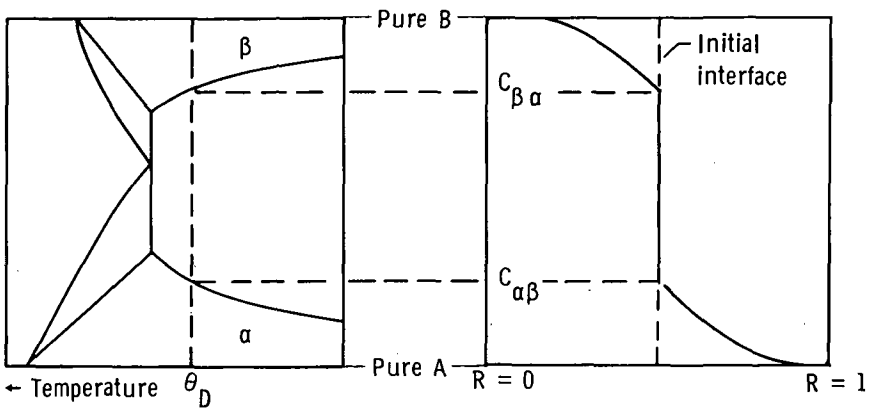

(b) Two phase - limited solid solubility.

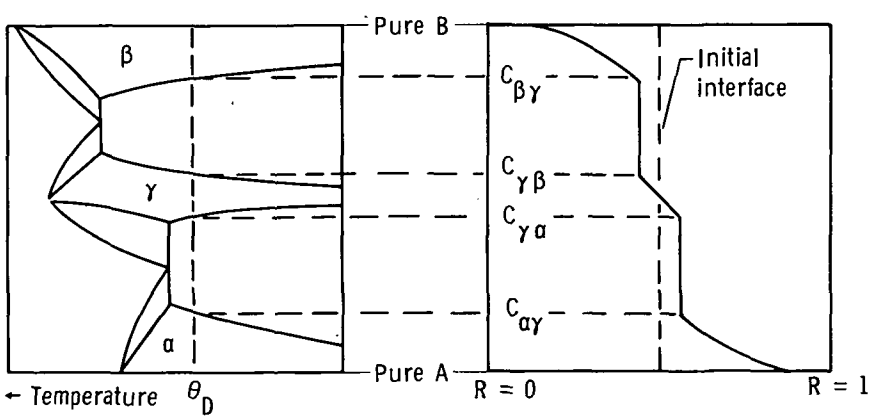

(c) Three phase - intermediate-phase formation.

Figure 1.- Phase diagrams and examples of concentration profiles produced by diffusion between initially pure A and pure B at temperature θ_D in single-, two-, and three-phase binary alloy systems.

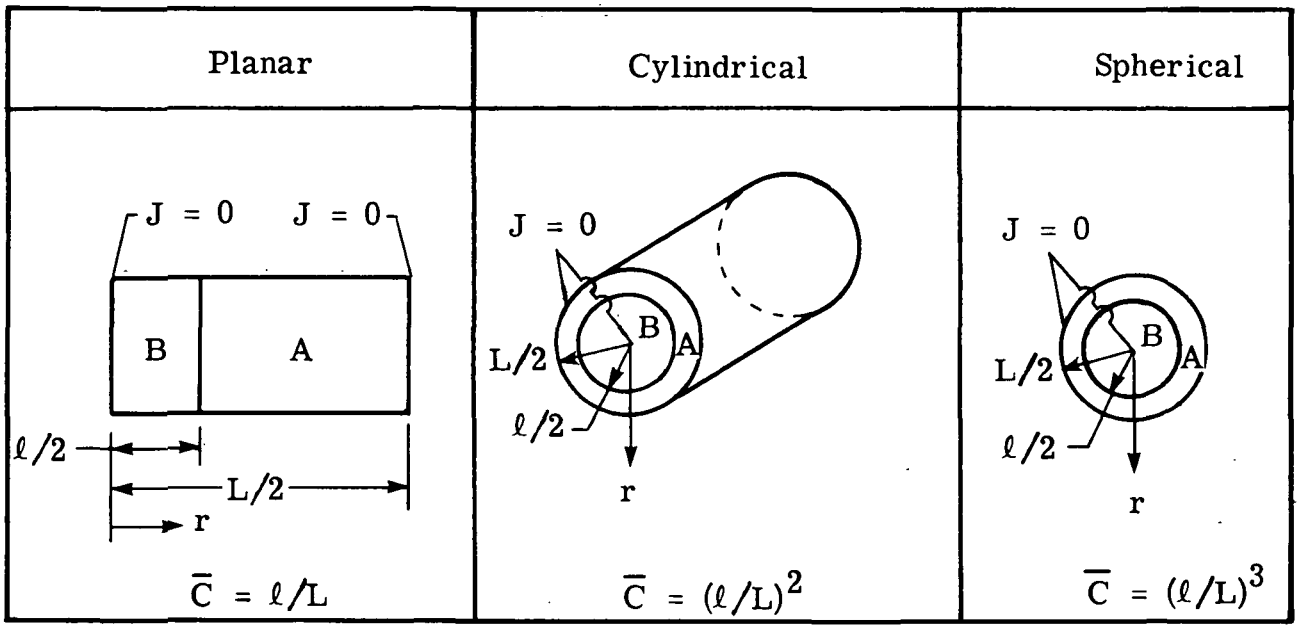

Figure 2.- Average composition, initial conditions, and zero-flux (J = 0) boundary conditions for different geometries.

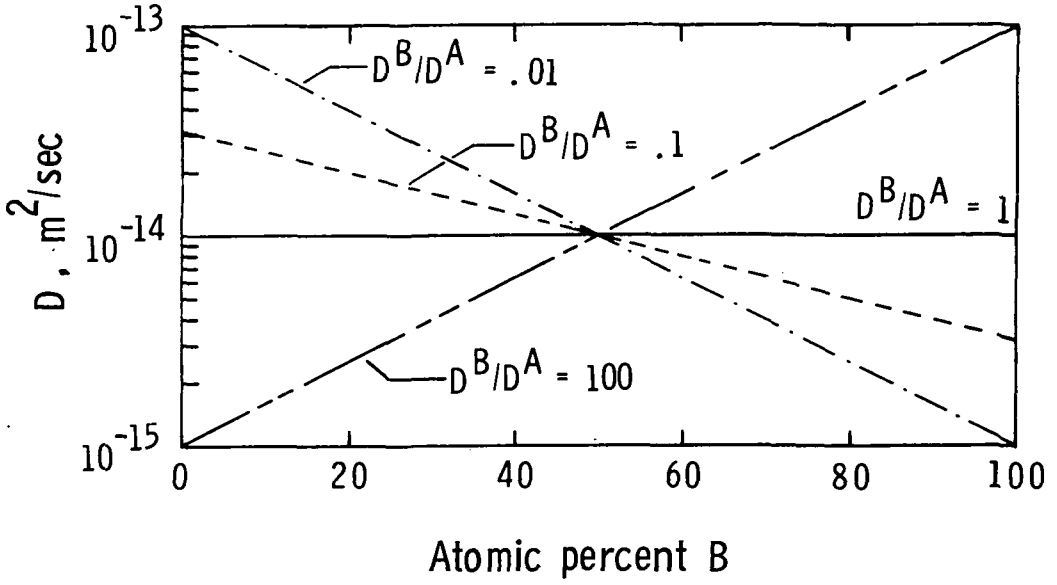

(a) D variations.

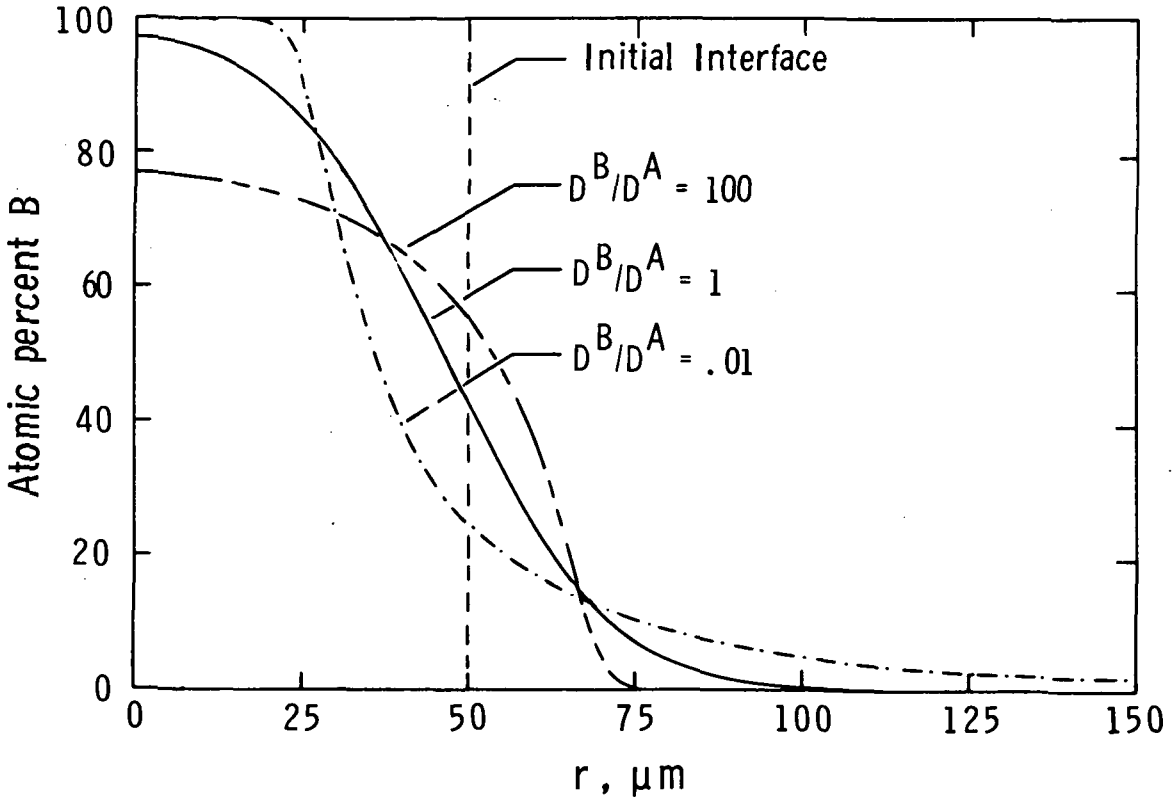

(b) Concentration profiles.

Figure 3.- Example of D variations in single-phase systems and associated concentration profiles in cylindrical couple with $\bar{C}$ = 0.111 at intermediate stage of diffusion (5 hr).

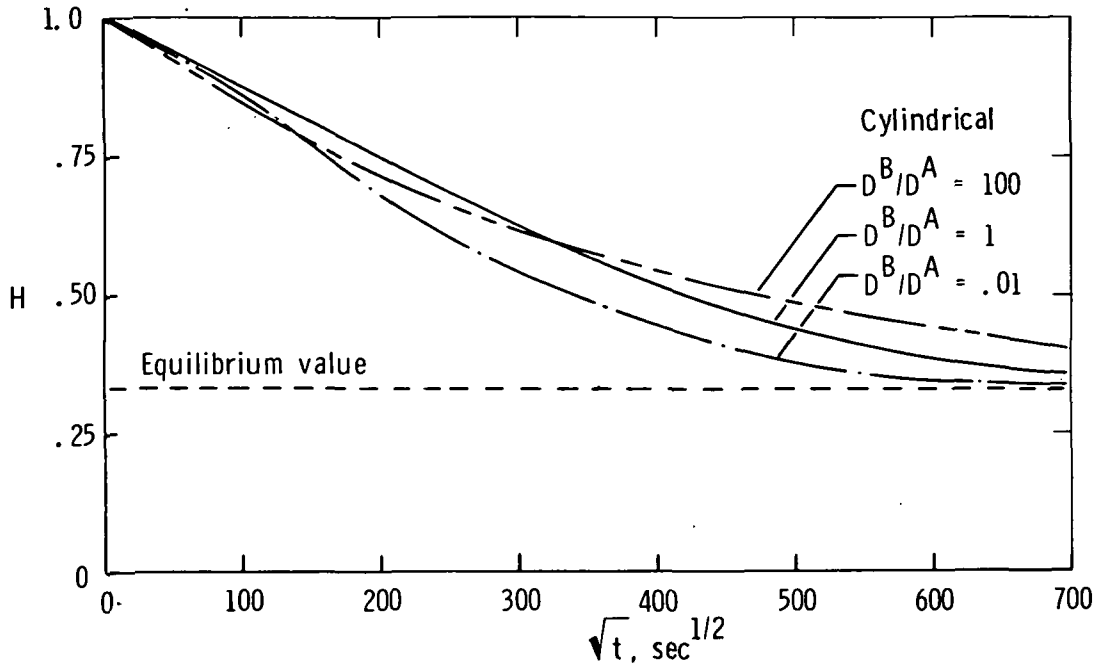

(a) D variation effects.

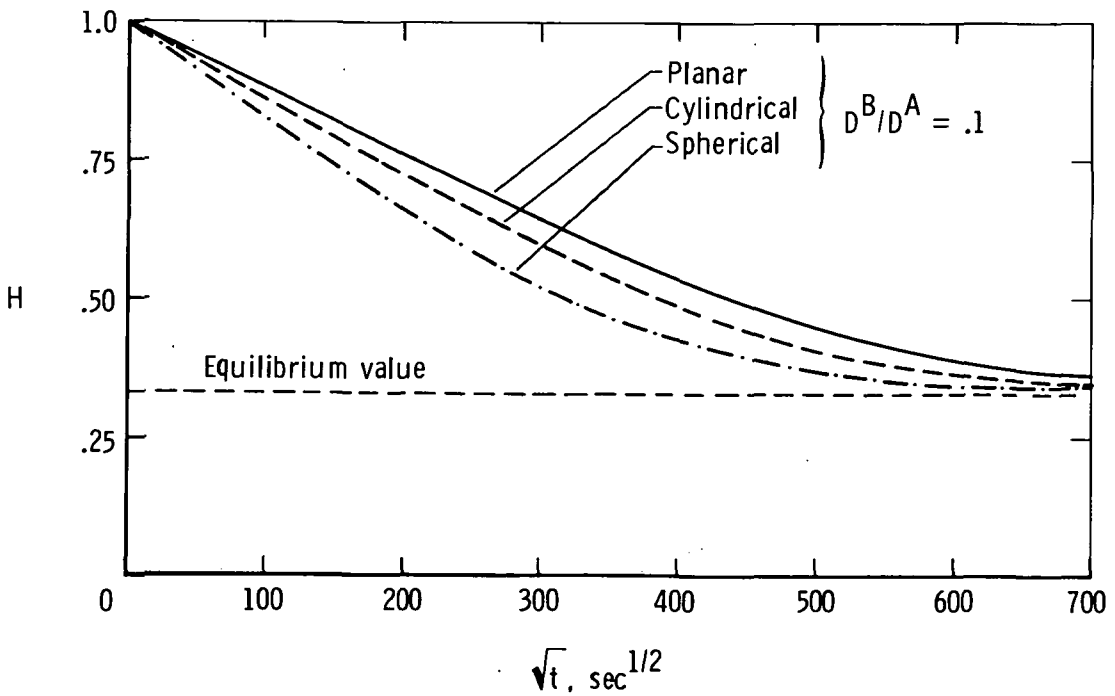

(b) Geometry effects.

Figure 4.- D variation and geometry effects on degree of homogenization for couples with $\bar{C}$ = 0.333 atomic fraction of B.

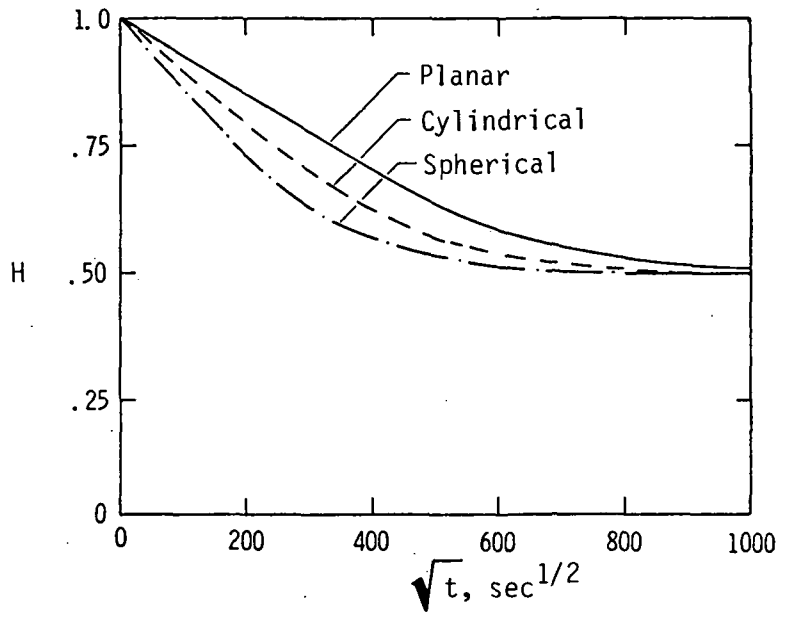

(a) $\bar{C}$ = 0.50.

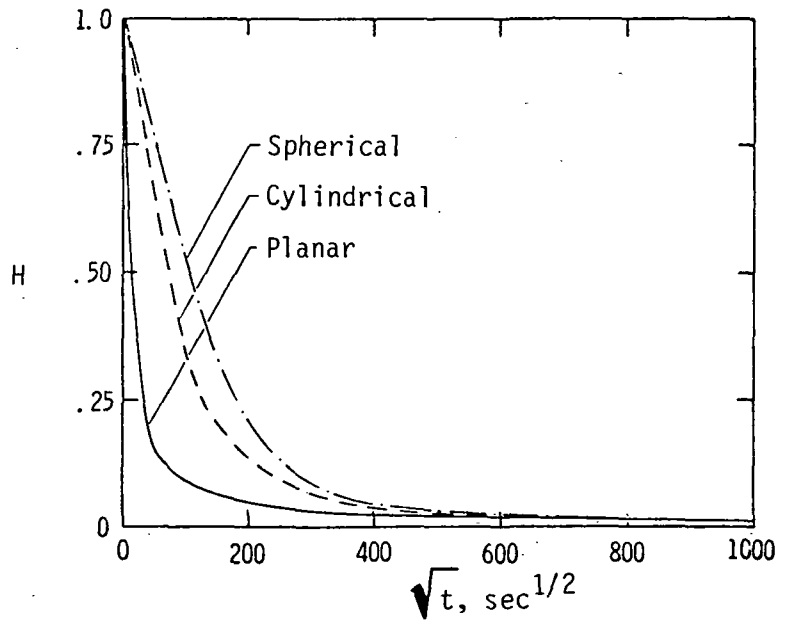

(b) $\bar{C}$ = 0.01.

Figure 5.- Average composition and geometry effects on degree of homogenization.

Planar		Cylindrical	Spherical
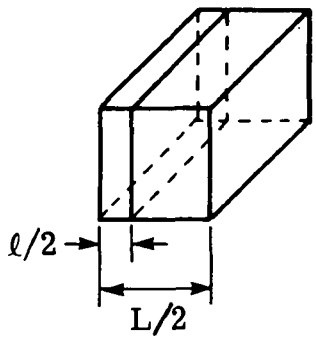		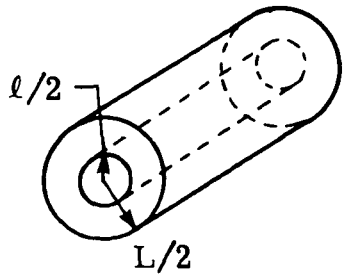	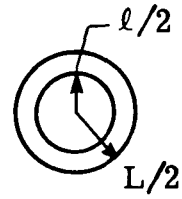
$\frac{s}{v} = \frac{1 \times 1}{\ell/2 \times 1 \times 1} = \frac{2}{\ell}$		$\frac{s}{v} = \frac{\pi\ \ell \times 1}{\pi\ (\ell/2)^2 \times 1} = \frac{4}{\ell}$	$\frac{s}{v} = \frac{\pi\ \ell^2}{4/3\ \pi\ (\ell/2)^3} = \frac{6}{\ell}$
$\bar{C} = (\ell/L)$		$\bar{C} = (\ell/L)^2$	$\bar{C} = (\ell/L)^3$
$\frac{s}{v} = \frac{2}{\bar{C}\ L}$		$\frac{s}{v} = \frac{4}{(\bar{C})^{1/2}\ L}$	$\frac{s}{v} = \frac{6}{(\bar{C})^{1/3}\ L}$
$\bar{C}$	$(s/v) \times L/2 = 1/\bar{C}$	$(s/v) \times L/2 = 2/(\bar{C})^{1/2}$	$(s/v) \times L/2 = 3/(\bar{C})^{1/3}$
.50	2.00	2.83	3.78
.01	100	20.0	13.9

Figure 6.- Dependence of s/v on geometry and $\bar{C}$.

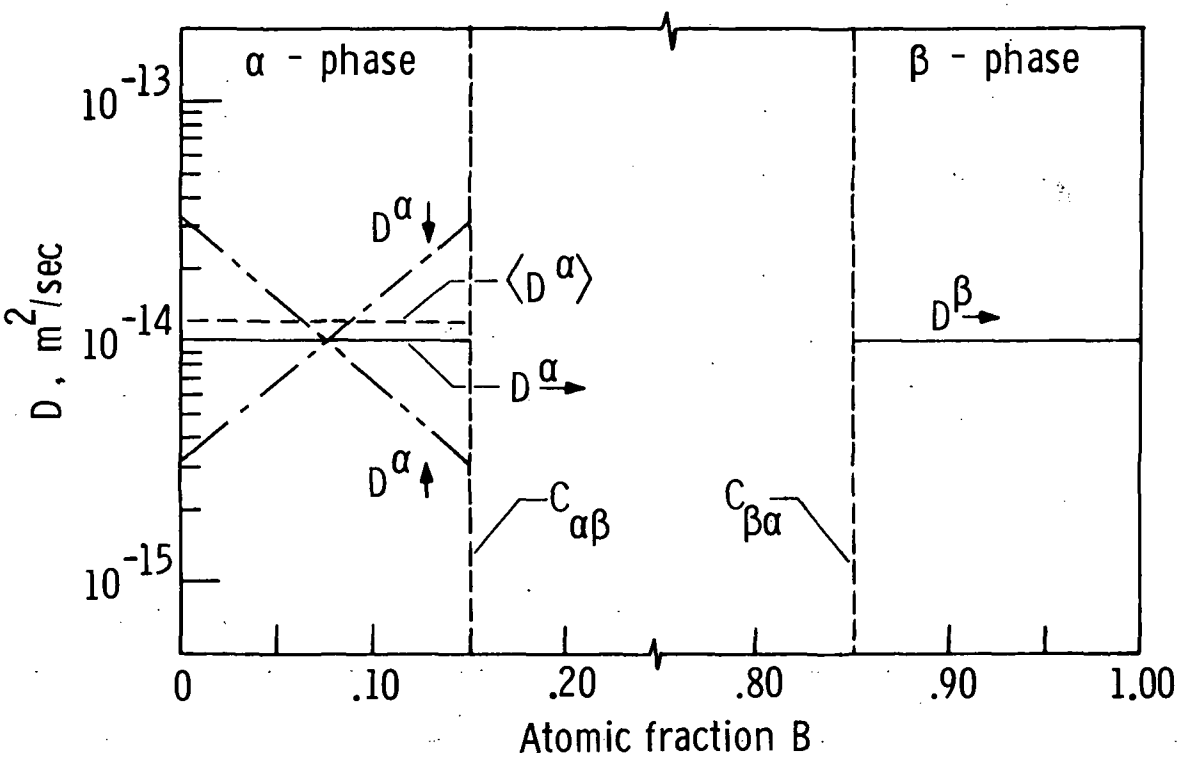

Figure 7.- Diffusion coefficient variations in α- and β-phases of two-phase binary alloy system.

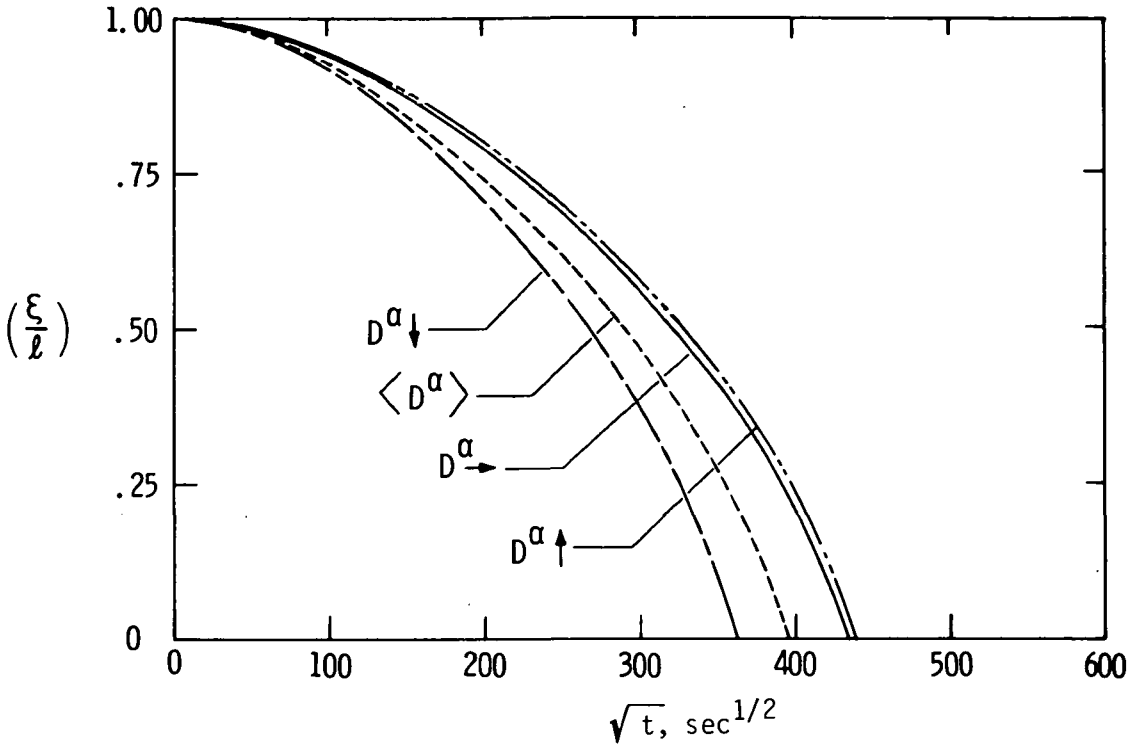

(a) Change in thickness of β-phase with diffusion time.

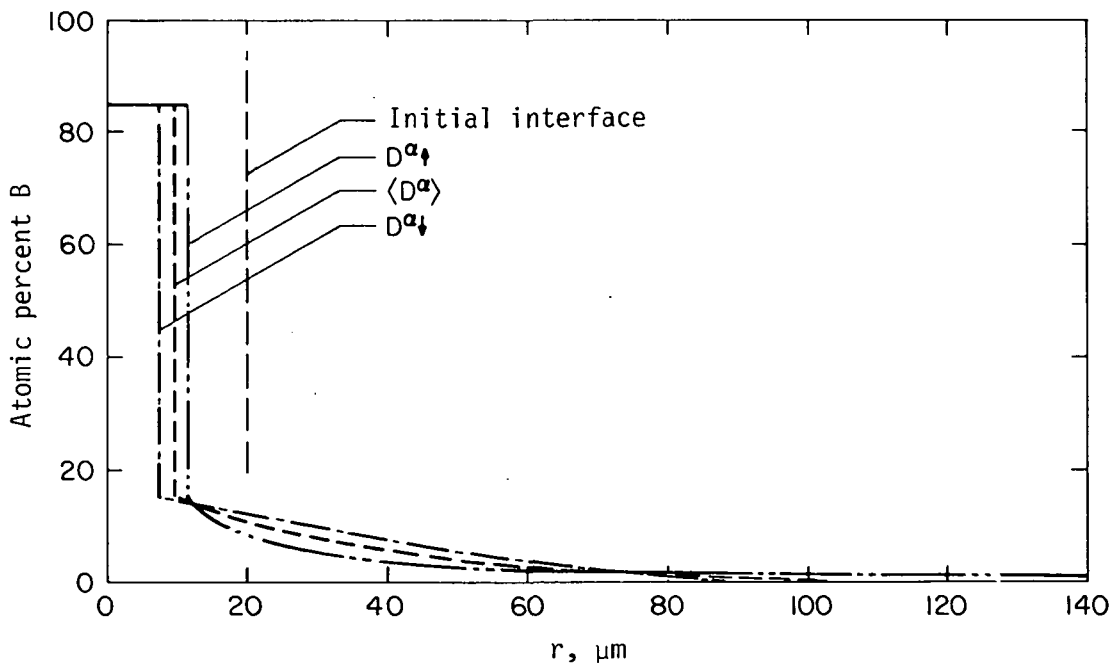

(b) Concentration profiles at $\sqrt{t}$ = 300 $sec^{1/2}$.

Figure 8.- Effect of D^{α} variations in cylindrical couple with $\bar{C}$ = 0.02 on β-phase thickness and composition profiles. Diffusion conditions correspond to cases 1, 2, 3, and 4 of table 3.

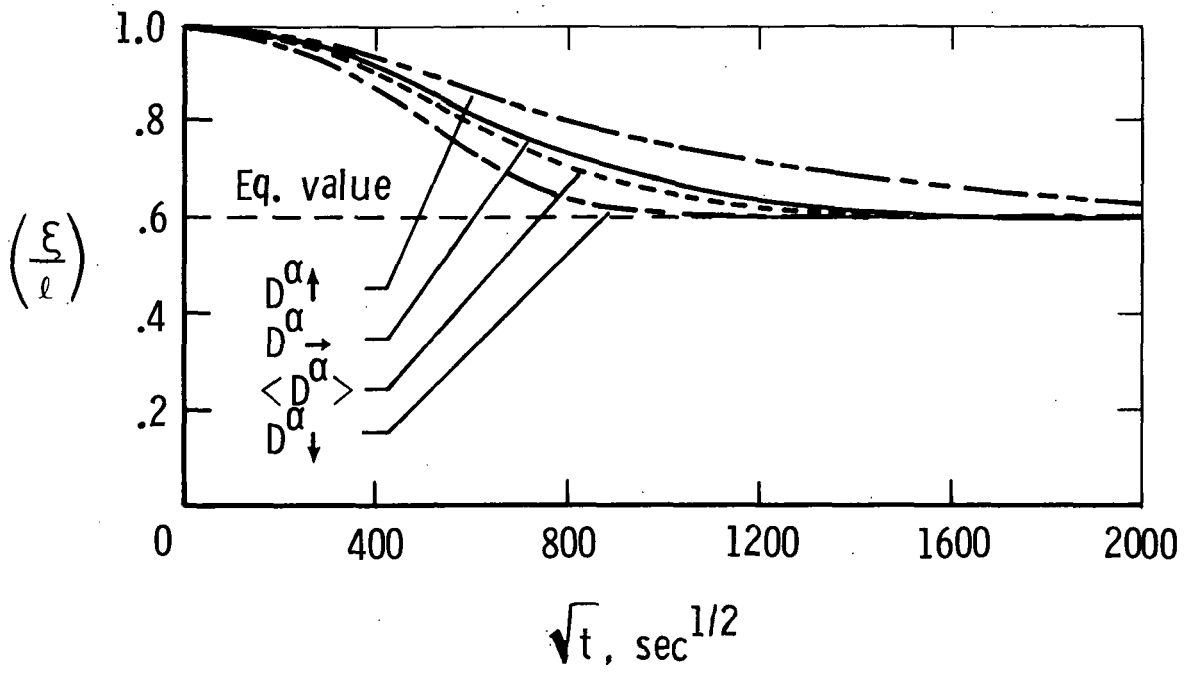

(a) Change in thickness of β-phase with diffusion time.

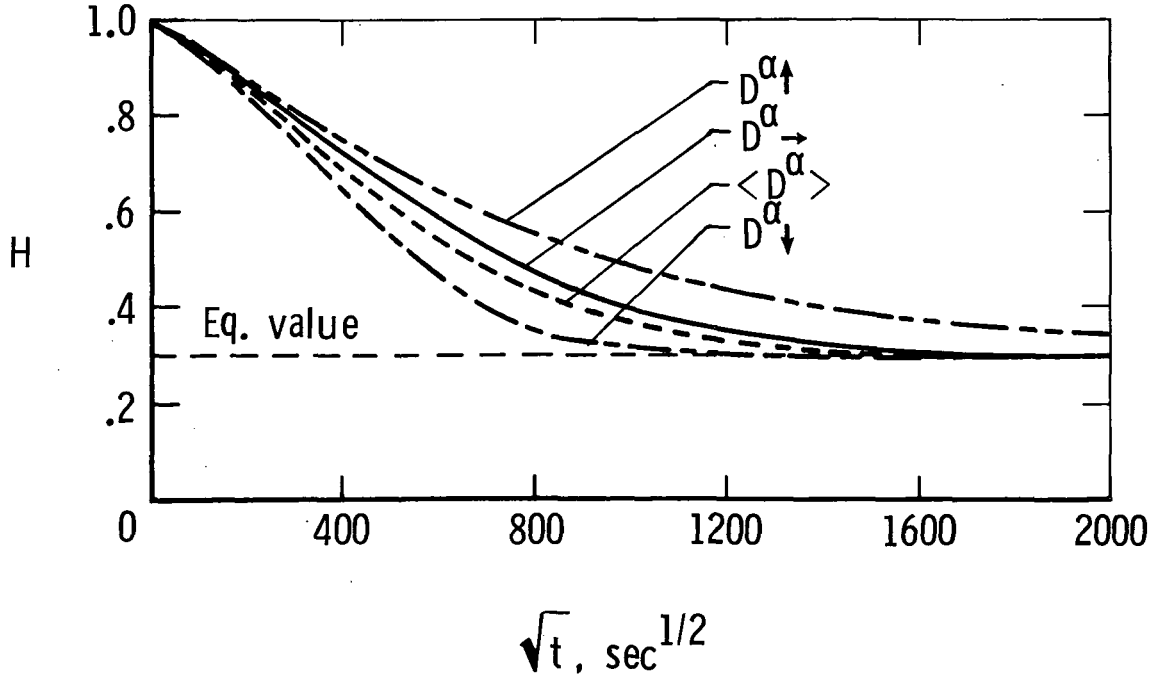

(b) Change in amount of B in β-phase with diffusion time.

Figure 9.- Effect of D^{α} variations in cylindrical couple with $\bar{C} = 0.20$. Diffusion conditions correspond to cases 5, 6, 7, and 8 of table 3.

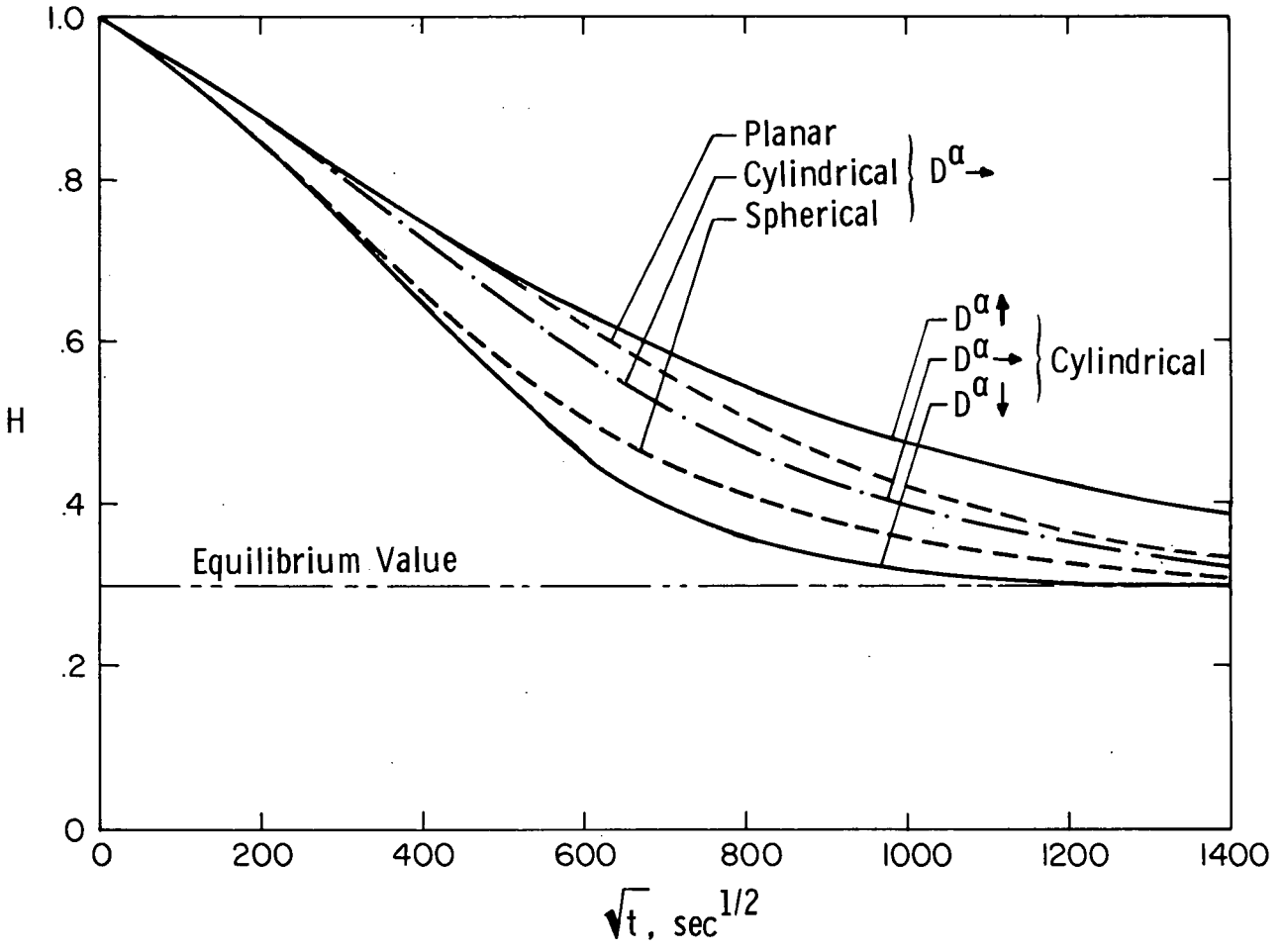

Figure 10.- Geometry and D variation effects on degree of homogenization. Diffusion conditions for D variation curves correspond to cases 5, 6, and 7 of table 3. Conditions for different geometry curves correspond to cases 7, 9, and 10 of table 3.

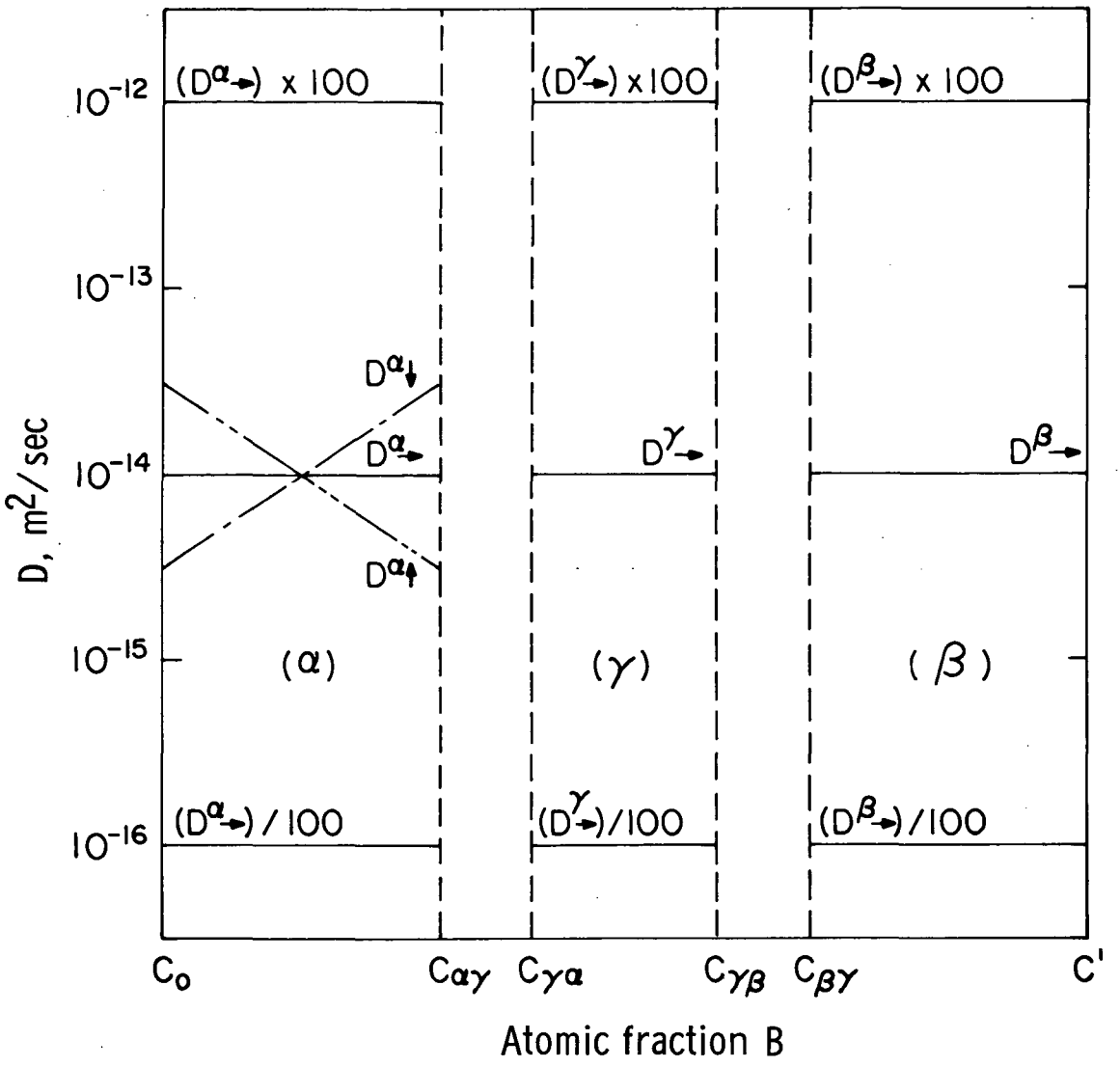

Figure 11.- Diffusion coefficient variation in α-, β-, and γ-phases of three-phase system.

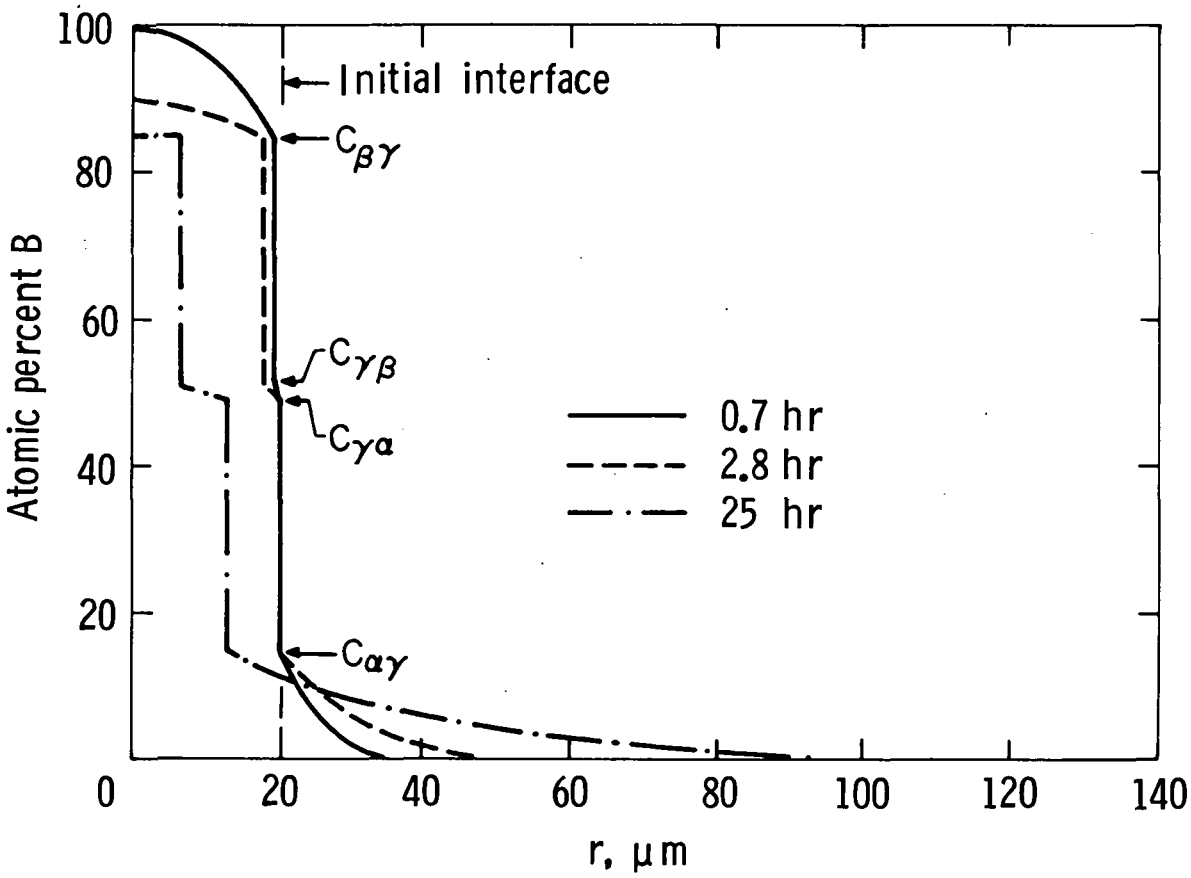

Figure 12.- Concentration profiles at different times in cylindrical couple with $\bar{C} = 0.02$. Diffusion conditions correspond to case 1 of table 4.

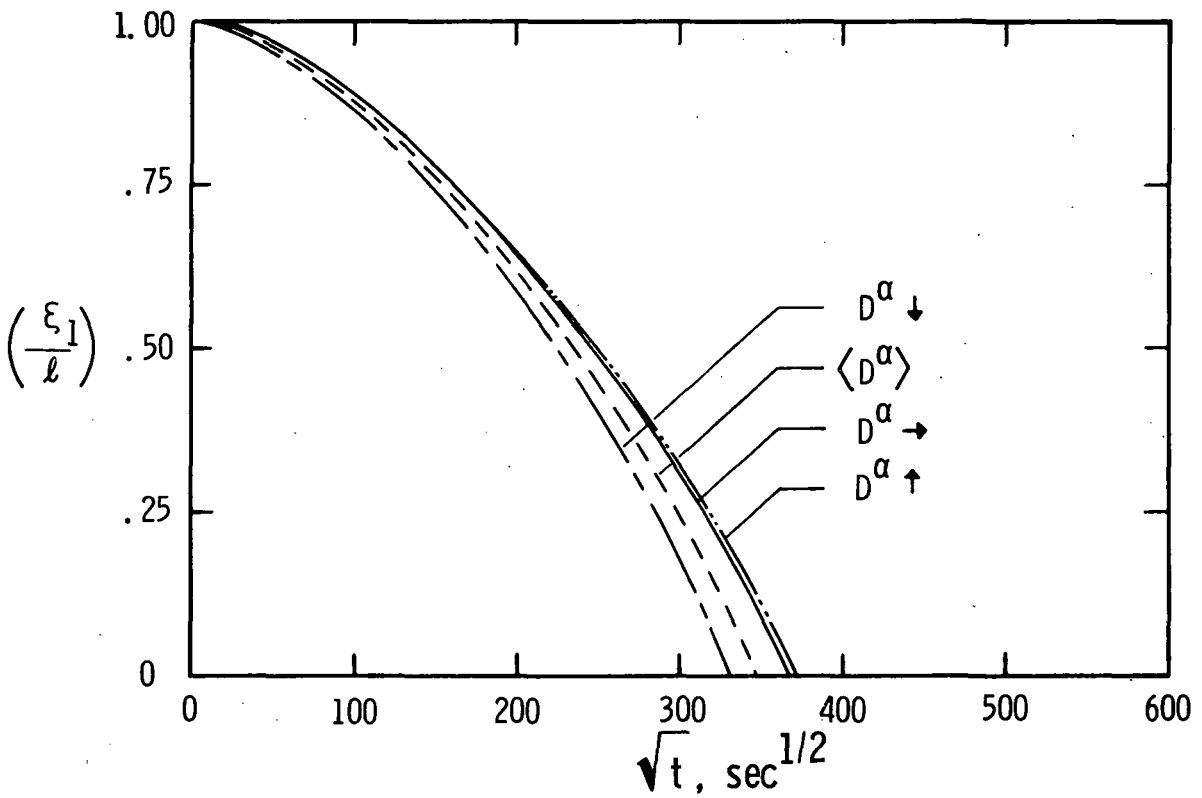

Figure 13.- Effect of D^{α} variations in cylindrical couple with $\bar{C} = 0.02$ on β-phase thickness. Diffusion conditions correspond to cases 1, 2, 3, and 4 of table 4.

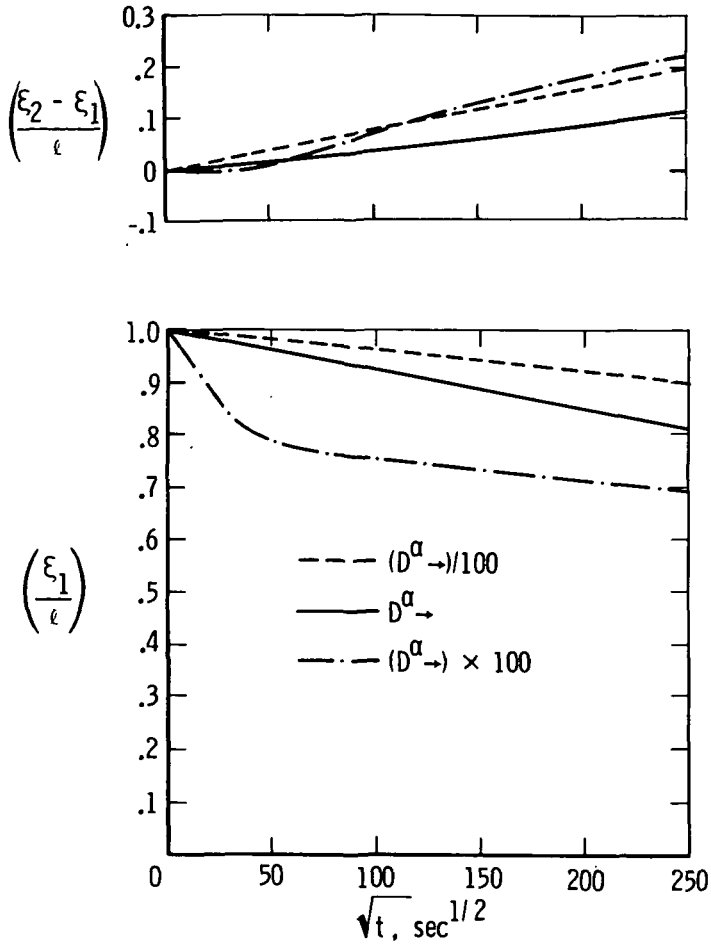

(a) Change in thickness of γ- and β-phases with diffusion time.

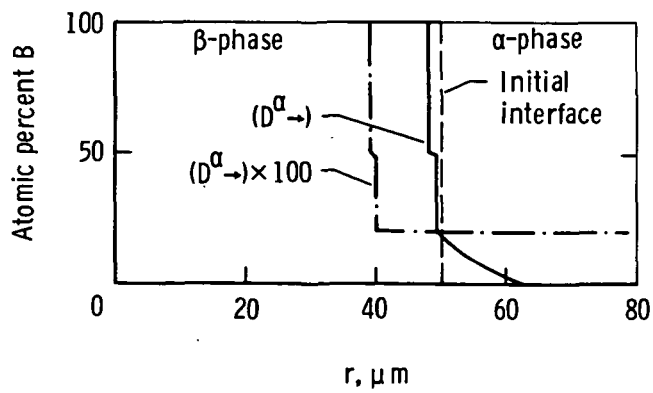

(b) Concentration profiles at $\sqrt{t}$ = 50 $sec^{1/2}$.

Figure 14.- Effect of D^{α} variations in cylindrical couple with $\bar{C}$ = 0.40 on γ- and β-phase thicknesses and concentration profiles. Diffusion conditions correspond to cases 5, 6, and 7 of table 4.

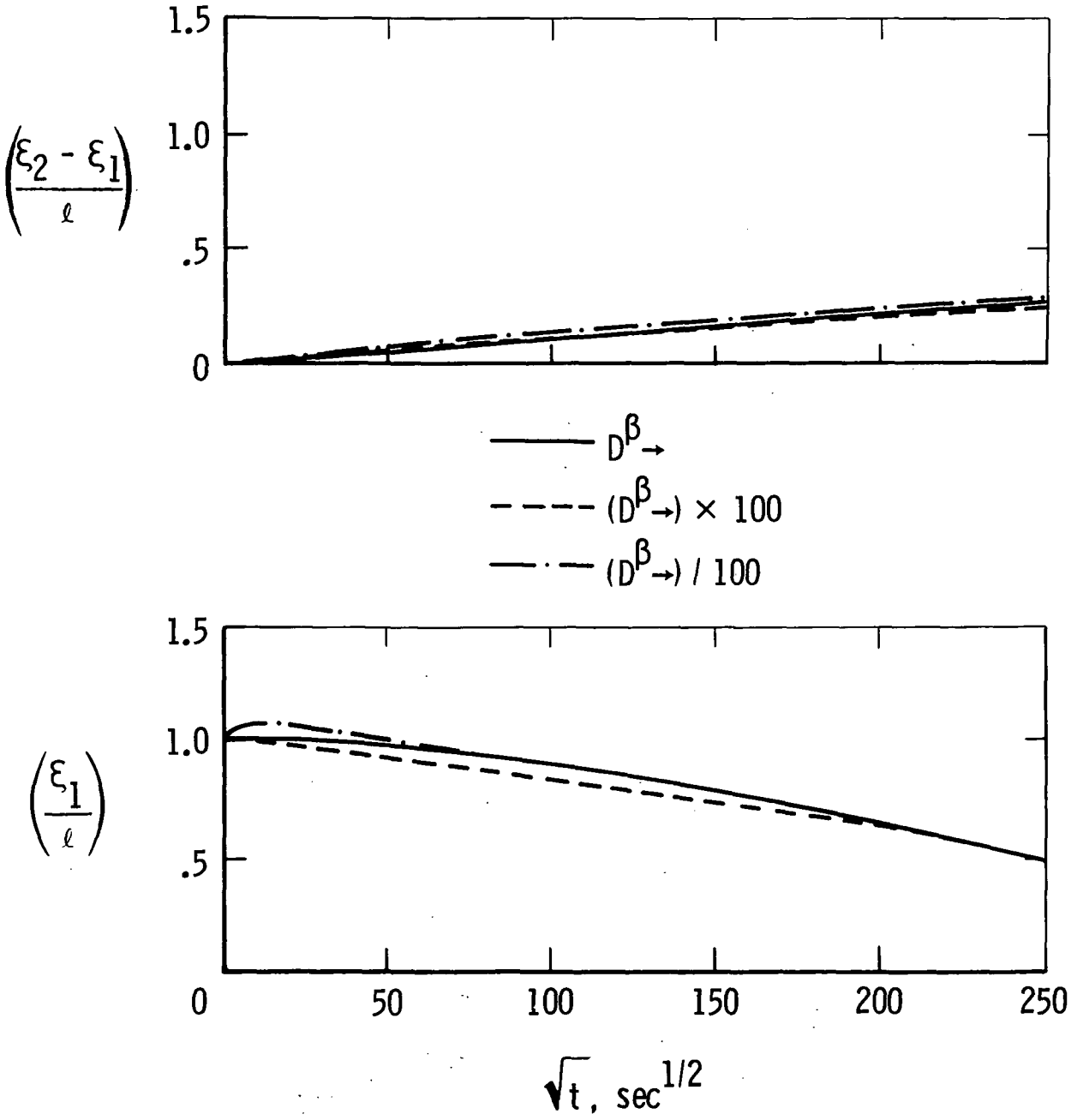

Figure 15.- Effect of large changes in D^{β} on γ- and β-phase thicknesses for cylindrical couple with $\bar{C} = 0.02$. Diffusion conditions correspond to cases 1, 8, and 9 of table 4.

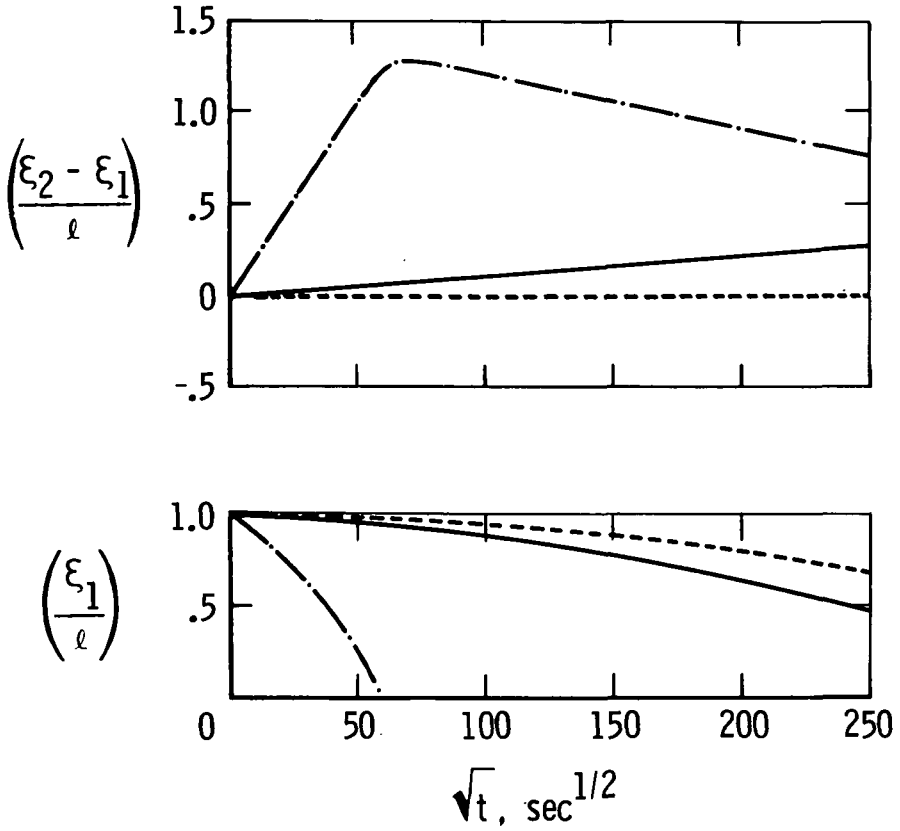

(a) Change in thickness of γ- and β-phases with diffusion.

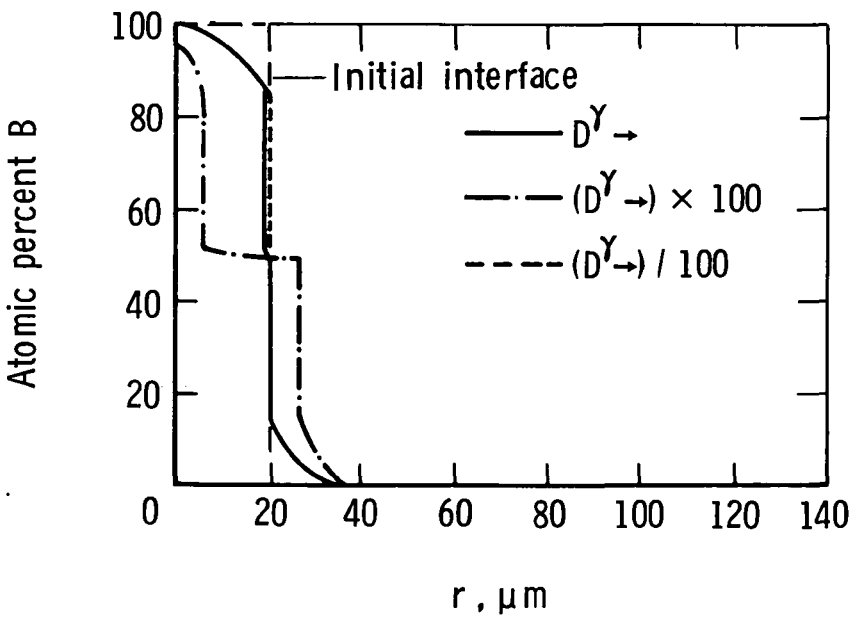

(b) Concentration profiles at $\sqrt{t} = 50\ sec^{1/2}$.

Figure 16.- Effect of large changes in D^{γ} for cylindrical couple with $\bar{C} = 0.02$ on γ- and β-phase thicknesses and concentration profiles. Diffusion conditions correspond to cases 1, 10, and 11 of table 4.

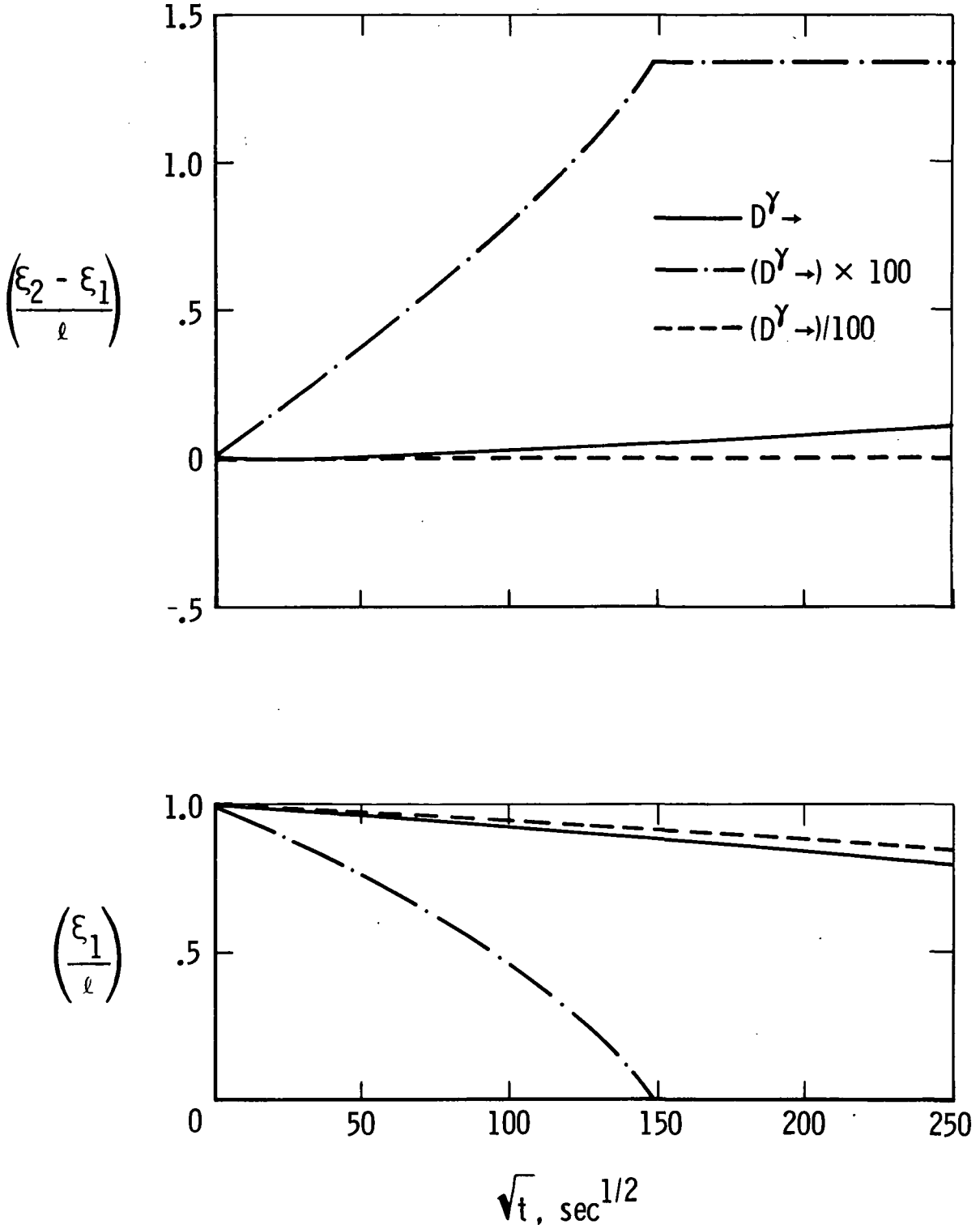

Figure 17.- Effect of large changes in D^{γ} on γ- and β-phase thicknesses for a cylindrical couple with $\bar{C} = 0.40$. Diffusion conditions correspond to cases 5, 12, and 13 of table 4.

1. Report No.	2. Government Accession No.	3. Recipient's Catalog No.
NASA TP-1281		

4. Title and Subtitle	5. Report Date
EFFECT OF CONCENTRATION DEPENDENCE OF THE DIFFUSION COEFFICIENT ON HOMOGENIZATION KINETICS IN MULTIPHASE BINARY ALLOY SYSTEMS	November 1978
	6. Performing Organization Code
7. Author(s)	8. Performing Organization Report No.
Darrel R. Tenney and Jalaiah Unnam	L-12224
	10. Work Unit No.
9. Performing Organization Name and Address	506-16-23-01
NASA Langley Research Center Hampton, VA 23665	11. Contract or Grant No.
	13. Type of Report and Period Covered
12. Sponsoring Agency Name and Address	Technical Paper
National Aeronautics and Space Administration Washington, DC 20546	14. Sponsoring Agency Code

15. Supplementary Notes

Darrel R. Tenney: Langley Research Center.
Jalaiah Unnam: The George Washington University, Joint Institute for Advancement of Flight Sciences, Langley Research Center.

16. Abstract

Diffusion calculations were performed to establish the conditions under which concentration dependence of the diffusion coefficient was important in single-, two-, and three-phase binary alloy systems. Finite-difference solutions were obtained for each type of system using diffusion coefficient variations typical of those observed in real alloy systems. Solutions were also obtained using average diffusion coefficients determined by taking a logarithmic average of each diffusion coefficient variation considered. The constant diffusion coefficient solutions were used as reference in assessing diffusion coefficient variation effects. Calculations were performed for planar, cylindrical, and spherical geometries in order to compare the effect of diffusion coefficient variations with the effect of interface geometries. In most of the cases considered, the diffusion coefficient of the major-alloy phase was the key parameter that controlled the kinetics of interdiffusion.

17. Key Words (Suggested by Author(s))	18. Distribution Statement
Diffusion in solids Concentration dependent diffusion Multiphase systems Alloy homogenization Binary alloys	Unclassified - Unlimited Subject Category 26

19. Security Classif. (of this report)	20. Security Classif. (of this page)	21. No. of Pages	22. Price*
Unclassified	Unclassified	36	$4.50

* For sale by the National Technical Information Service, Springfield, Virginia 22161

NASA-Langley, 1978

National Aeronautics and
Space Administration

Washington, D.C.
20546

Official Business
Penalty for Private Use, $300

THIRD-CLASS BULK RATE

Postage and Fees Paid
National Aeronautics and
Space Administration
NASA-451

U.S.MAIL

NASA

POSTMASTER: If Undeliverable (Section 158 Postal Manual) Do Not Return